[AMERICAN JOURNAL OF SCIENCE, VOL. 295, JUNE, 1995, P. 742–786]

ABNORMAL PRESSURES AS HYDRODYNAMIC PHENOMENA

C. E. NEUZIL
U.S. Geological Survey,
431 National Center
Reston, Virginia 22092

ABSTRACT. So-called abnormal pressures, subsurface fluid pressures significantly higher or lower than hydrostatic, have excited speculation about their origin since subsurface exploration first encountered them. Two distinct conceptual models for abnormal pressures have gained currency among earth scientists. The static model sees abnormal pressures generally as relict features preserved by a virtual absence of fluid flow over geologic time. The hydrodynamic model instead envisions abnormal pressures as phenomena in which flow usually plays an important role. In this paper I develop the theoretical framework for abnormal pressures as hydrodynamic phenomena, show that it explains the manifold occurrences of abnormal pressures, and examine the implications of this approach.

Abnormal pressures can be explained as occurring in flow regimes that are both equilibrated and disequilibrated hydrodynamically. The former are "adjusted" to their geologic and hydrologic surroundings while the latter are not. Equilibrium-type abnormal pressures generally result from topographically-driven flow (as in artesian basins) but may also occur as a result of osmosis or fluid density contrasts. The more common and varied disequilibrium-type abnormal pressures are caused by natural geologic processes such as compaction, diagenesis, and deformation. These processes have the effect of distributed fluid sources or sinks and are manifested either as actual fluid sources/sinks or as virtual ones involving changing porosity and/or temperature. Disequilibrium-type abnormal pressures can be characterized in terms of three quantities: the size and permeability of their domains and the vigor of the "geologic forcing" or magnitude of the source/sink term. Published estimates reveal a surprising number of distinct geologic processes that can generate forcing sufficient to maintain abnormal pressures in dynamic systems. This observation is crucial to understanding why abnormal pressures need not indicate regimes that have been static over geologic time.

Low-permeability regions play key roles in both equilibrium- and disequilibrium-type abnormal pressures. Extensive low-permeability strata are generally required to generate abnormal pressures in topographically-driven flow regimes, while osmotically-driven flow and hydrodynamic disequilibrium occur only within regions composed of or encompassed by low-permeability media. Analyzing abnormal pressures as hydrodynamic phenomena often allows these low permeabilities to be estimated, something that is otherwise difficult to do. In some instances hydrodynamic analyses also shed light on rates of geologic processes and a region's geologic history.

NOTATION

c	solute concentration $[M/L^3]$.
g	gravitational acceleration $[L/T^2]$.
h	hydraulic head $[L]$.
h_D	dimensionless head, equal to h/l.
l	representative length; characteristic flow length $[L]$.
m	fluid mass $[M]$.
n	porosity $[L^3/L^3]$.
$\mathbf{q}$	specific flux of pore fluid $[L^3/L^2T]$.
t	time $[T]$.
t_D	dimensionless time, equal to $\kappa t/S_s' l^2$.
J	fluid source or sink $[M/L^3T]$.
K	bulk modulus of porous medium $[M/T^2L]$.
K_f	bulk modulus of fluid $[M/T^2L]$.
K_s	bulk modulus of porous medium solids $[M/T^2L]$.
P	fluid pressure $[M/T^2L]$.
R_d	sedimentary deposition rate $[L/T]$.
S_s'	specific storage $[L^{-1}]$.
T	temperature [degrees].
α_{Tf}	bulk thermal expansivity of fluid [degrees^{-1}].
α_{Tp}	bulk thermal expansivity of pores [degrees^{-1}].
$\dot{\epsilon}$	volumetric strain rate $[T^{-1}]$.
ζ_m	mechanical loading efficiency $[T^2L/M]$.
ζ_T	thermal loading efficiency [degrees^{-1}].
κ	hydraulic conductivity $[L/T]$.
κ_c	chemical osmotic conductivity $[L^2/T]$.
ξ	coefficient relating bulk volumetric strain to porosity loss, equal to $1 - (K/K_s)$ [dimensionless].
ρ	density of pore fluid $[M/L^3]$.
σ_t	mean total stress $[M/T^2L]$.
Γ	geologic forcing $[L^3/L^3T]$.
Γ_D	dimensionless geologic forcing, equal to $(l/\kappa)\Gamma$.
∇_D^2	dimensionless Laplacian operator, equal to $l^2\nabla^2$.
$(\ )^*$	indicates a process occurring during diagenesis/metamorphism.

INTRODUCTION

Abnormal subsurface fluid pressures (defined here as differing from hydrostatic by more than 100 m of hydraulic head) are conspicuous natural phenomena that dramatically affect drilling and the extraction of subsurface fluids. Most direct knowledge of abnormal pressures comes from hydrocarbon exploration, and the phenomenon typically has been associated with thick sedimentary accumulations in deep basins (for example, see Fertl, 1976). However, it is becoming clear that abnormal pressures exist in many different geologic settings. For example, they have also been detected in shallow strata, and there is evidence that they exist in environments as diverse as accretionary prisms and continental shields. The host formations range from unconsolidated sediments to crystalline rocks at many kilometers depth and can be as old as Precambrian and as young as Pleistocene.

Since their discovery, researchers have sought to determine how abnormal pressures originate and what they reveal about subsurface fluid regimes and geologic environments. Investigators have generally followed one of two distinct conceptual approaches to abnormal pressures. Containment of pore fluids by essentially impermeable geologic units has often been appealed to, either explicitly or implicitly. This line of reasoning explains abnormal pressures as static phenomena that owe their existence to a virtual absence of fluid fluxes. The idea is explicitly stated by Hunt (1990), who argues that abnormal pressures are maintained by barriers to flow that "... prevent essentially all pore fluid movement over substantial intervals of geologic time." The same idea has also been outlined by Powley (1990), who describes abnormal pressure regimes as static and occurring where the subsurface is compartmentalized by impermeable barriers to fluid flow. In a similar vein, Bradley (1975) has suggested that pressures can be preserved substantially unchanged as their geologic framework evolves. In a very real sense, the static conceptualization envisions abnormal pressures as relict features.

The other conceptual approach to abnormal pressures might be termed the hydrodynamic model. A number of investigators, such as Hubbert and Rubey (1959), Bredehoeft and Hanshaw (1968), Sharp and Domenico (1976), and Bethke (1989), to name only a few, have implicitly utilized this approach in their analyses of various abnormal pressure regimes. From this perspective, abnormal pressures generally are seen as dynamic rather than static, in most cases representing a balance between ongoing geologic processes that perturb the pressure and fluid fluxes that tend to dissipate the perturbations. Where geologic processes do not play an active role, abnormal pressures are usually seen simply as manifestations of flow driven by topography (sometimes called gravity-driven flow). Only under certain circumstances, involving osmosis or fluids of differing densities, are abnormal pressures expected under static conditions.

Although the hydrodynamic approach to abnormal pressures has been used by many researchers, it has never been synthesized into a single, general theoretical framework. In addition, the implications of the hydrodynamic model seem not to be widely, or fully, appreciated. In this paper I develop a generic hydrodynamic model for abnormal pressures, use it to examine the validity of the hydrodynamic approach, and explore its ramifications. Specifically, the paper (1) describes the natural hydrodynamic mechanisms that may give rise to abnormal pressures, (2) shows that, in view of the properties and behavior of the crust as presently understood, these mechanisms can create and maintain abnormal pressures (citing specific examples), and (3) considers what our observations then allow us to deduce about flow, permeability, and geologic processes at various scales. An important outcome of these efforts is identification of commonalities shared by abnormal pressure regimes that are seemingly very different. Hopefully, the resulting perspective is a useful one.

CONCEPTUAL BASIS

For the task at hand, a useful description of subsurface flow must incorporate the various natural mechanisms that can affect pressure. Bredehoeft and Norton (1990) have enumerated many of these, and in this section I develop a description that accounts for them explicitly. At the generic level of description required here, this task is not too difficult, because there are relatively few ways in which the natural environment can supply pressure energy to pore fluids.

To simplify the development, I will not account for large deformations of the porous matrix or rigorously describe the coupling between fluid pressure changes and three-dimensional deformation of the solid matrix using poroelasticity. Also, I will consider only fluid transport and not that of heat or solutes. These simplifications do not impair analysis of the relevant processes or affect the conclusions and can be relaxed when necessary (for example, see Rice and Cleary, 1976, and Bethke, 1989). Finally, I will for the most part ignore heterogeneity in fluid density and treat all fluids as a single phase. Although many abnormal pressure regimes contain separate hydrocarbon phases, the abnormal pressuring usually does not result from density differences or the presence of non-water phases *per se* (for example, see Hubbert and Rubey, 1959; Spencer, 1987). In this sense, the approach adopted here addresses many of the questions raised by Hunt (1990).

The energy to generate pressures and drive flow in the subsurface is derived from one or more of the following: topographic elevation, chemical potential gradients, porosity changes, temperature changes, and fluid sources. I begin by considering actual fluid sources which, in the subsurface, can arise from a number of natural physico-chemical processes, generally as rock or sediments are heated and compressed. Examples include petroleum generation (Bredehoeft, Wesley, and Fouch, 1994) and devolatilization of minerals (Walther and Orville, 1982). These processes are generally part of a suite of changes we refer to as diagenesis or metamorphism and commonly are accompanied by changes in porosity and thermomechanical effects on the fluid and solid.

Geologic fluid sources generally are distributed, meaning that they are present throughout a volume of rock, although their strength (the rate of fluid production) may vary spatially. In the presence of a distributed fluid source of strength J, the equation for fluid mass balance in a porous medium is written as

$$\frac{\partial}{\partial t}(\rho n) + \nabla \cdot (\rho \mathbf{q}) - J = 0 \qquad (1)$$

where ρ is fluid density, n is porosity, and $\mathbf{q}$ is the specific flux of pore fluid. J has the dimensions M/L^3T and represents the mass of fluid added to a volume of rock per time by diagenetic or metamorphic processes. It is balanced by accumulation of fluid mass described by the first term and loss or gain of fluid mass by flow described by the second term.

Next, porosity and temperature changes must be considered. The change in fluid mass $m = \rho n$ in the first term of (1) can be written as

$$dm = nd\rho + \rho dn, \tag{2}$$

showing that it arises from changes in both fluid density and porosity. In the subsurface, porosity is affected by many different geologic mechanisms, including changes in effective stress. The latter result when external loads change, as during burial or tectonic compression, and when fluid pressure changes (Biot, 1941). Heating and cooling, which cause the solid matrix to deform thermomechanically, also change the porosity (Palciauskas and Domenico, 1982). In other instances, porosity changes when solid components are lost by conversion to fluids (as in petroleum generation from solid kerogen and smectite dewatering), or when the porous structure collapses as a result of such processes (Stephenson, Plumley, and Palciauskas, 1992). Finally, other diagenetic processes, including plastic deformation of the solid skeleton (Šuklje, 1969), pressure solution (Palciauskas and Domenico, 1989; Gratz, 1991), and other mineral dissolution and precipitation processes (Land, 1991) also effect significant changes in porosity. Following the approach used by Neuzil (1993), these mechanisms can be described by

$$dn = -\left(\frac{1}{K} - \frac{1}{K_s}\right)d\sigma_t + \left(\frac{1}{K} - \frac{1}{K_s} - \frac{n}{K_s}\right)dP + n\alpha_{Tp}dT + (dn)^*, \tag{3}$$

where K and K_s are elastic bulk moduli of the porous medium and solid grains, σ_t is total stress, P is fluid pressure, T is temperature, and α_{Tp} is the bulk thermal expansivity of the pore structure. The first two terms describe the effect of external stress and fluid pressure changes, and the third term describes thermoelastic effects. The last term lumps together, without explicitly describing them, the diagenetic and metamorphic processes that affect porosity.

As noted by Domenico and Palciauskas (1979), fluid density depends on pressure and temperature through

$$d\rho = \frac{\rho}{K_f}dP - \rho\alpha_{Tf}dT, \tag{4}$$

where K_f is the fluid bulk modulus, and α_{Tf} its bulk thermal expansivity. Although (4) is approximate for large pressure and temperature changes, it can be used here without introducing undue error. Substituting (3) and (4) into (2) gives

$$dm = d\rho n = -\rho\left(\frac{1}{K} - \frac{1}{K_s}\right)d\sigma_t + \rho\left[\left(\frac{1}{K} - \frac{1}{K_s}\right) + \frac{n}{K_f} - \frac{n}{K_s}\right]dP - \rho n(\alpha_{Tf} - \alpha_{Tp})dT + \rho(dn)^* \quad (5)$$

as a statement of the accumulation of fluid mass in a volume of rock. Substituting (5) into (1) and recalling that ρ is assumed to be spatially constant, we obtain

$$-\nabla \cdot \mathbf{q} = -\left(\frac{1}{K} - \frac{1}{K_s}\right)\frac{\partial \sigma_t}{\partial t} + \left[\left(\frac{1}{K} - \frac{1}{K_s}\right) + \frac{n}{K_f} - \frac{n}{K_s}\right]\frac{\partial P}{\partial t} + n(\alpha_{Tp} - \alpha_{Tf})\frac{\partial T}{\partial t} + \left(\frac{\partial n}{\partial t}\right)^* - \frac{J}{\rho}. \quad (6)$$

Converting fluid pressure to hydraulic head and consolidating terms gives

$$-\nabla \cdot \mathbf{q} = -\zeta_m \frac{\partial \sigma_t}{\partial t} + S'_s \frac{\partial h}{\partial t} - \zeta_T \frac{\partial T}{\partial t} + \left(\frac{\partial n}{\partial t}\right)^* - \frac{J}{\rho}, \quad (7)$$

where $\zeta_m = K^{-1} - K_s^{-1}$ is a mechanical loading efficiency, $\zeta_T = n(\alpha_{Tf} - \alpha_{Tp})$ is a thermal loading efficiency, and $S'_s = \rho g[(K^{-1} - K_s^{-1}) + n(K_f^{-1} - K_s^{-1})]$ is specific storage. The loading efficiencies represent the fraction of mechanical and thermal loading expressed as a change in fluid pressure.

We are now in a position to include the effects of topography (through hydraulic head) and chemical potential (through solute concentration) on the flow. Darcy's law relates the specific flux $\mathbf{q}$ through a porous medium to hydraulic driving forces. However, additional forces can also drive flow, and one of these, chemical potential, may be of significance for abnormal pressures. Temperature and electrical potential gradients sometimes drive pore fluid flow, but these seem to be insignificant effects in natural environments (Neuzil, 1986). A modified form of Darcy's law, which includes chemical driving forces in addition to hydraulic, can be written as

$$\mathbf{q} = -\kappa\nabla h + \frac{\kappa_c}{c}\nabla c \quad (8)$$

(Greenberg, 1971; Olsen, 1972), where c is the concentration of dissolved salts, κ is the hydraulic conductivity, and κ_c is the osmotic conductivity. Both κ and κ_c are tensor quantities that change when formation porosity changes, but for simplicity I will consider them to be scalar constants.

Substituting (8) into (7) we obtain

$$\nabla \cdot \left(\kappa \nabla h - \frac{\kappa_c}{c} \nabla c\right) = S'_s \frac{\partial h}{\partial t} + \Gamma \tag{9}$$

as the flow description we seek. The quantity Γ is here termed the geological forcing, defined as

$$\Gamma = -\zeta_m \frac{\partial \sigma_t}{\partial t} + \left(\frac{\partial n}{\partial t}\right)^* - \zeta_T \frac{\partial T}{\partial t} - \frac{J}{\rho}. \tag{10}$$

The first two terms on the right hand side of (10) account for the effects of stress changes and diagenesis/metamorphism, respectively, on porosity. The third term accounts for the thermomechanical response of both the fluid and solid matrix and the last term represents actual fluid sources and sinks. Eq (9) is similar to the pressure diffusion equation often used to describe flow in porous media but differs by including osmotic driving forces and geological forcing.

ABNORMAL PRESSURE IN EQUILIBRATED SYSTEMS

I will first consider the forms of abnormal pressure that can be explained by the simplest hydrodynamics, namely those largely unaffected by geological forcing Γ. Although Γ is never zero, its influence on the fluid pressures and flow will be insignificant when the system is relatively permeable or Γ is relatively small, or both. In these instances Γ is overwhelmed by the other terms in (9). In the absence of other disturbances, such as changing boundary conditions or human activity, the flow remains adjusted to its geologic setting and simply reflects the driving forces inherent in that environment; hydrodynamic transients do not exist. Although such systems are transient in the sense that they evolve with their environment over geologic time, the pressure pattern and flow can be understood completely in the context of the current state of the system and without regard to its history. Under these conditions, (9) simplifies to

$$\nabla \cdot \left(\kappa \nabla h - \frac{\kappa_c}{c} \nabla c\right) = 0. \tag{11}$$

In many cases the chemical driving forces can be ignored; significant salinity gradients may not exist, or, more frequently, rocks with osmotic membrane properties are not present, and κ_c is essentially zero. Eq (11) then becomes

$$\nabla \cdot (\kappa \nabla h) = 0. \tag{12}$$

Topographically-driven Flow

It has been recognized that topographically-driven flow, which is governed by (12), produces pressures that depart from hydrostatic, although often not dramatically. A classic analysis of topographically-driven flow was made by Tóth (1963) and later extended by Freeze and Witherspoon (1967) to heterogeneous and anisotropic domains. Hitchon (1969a,b) first demonstrated that topographically-driven flow could actually explain certain patterns of hydraulic head observed in heterogeneous rocks. These pioneering studies showed the tendency for subhydrostatic pressures in topographically elevated areas and superhydrostatic pressures in topographically low areas.

Non-hydrostatic conditions in topographically-driven flow can be strongly amplified by low-permeability zones to produce conspicuous abnormal pressures. Examples of this phenomenon have been recognized for more than a century because of the flowing water wells they have provided. Artesian groundwater systems such as Australia's Great Artesian Basin (Habermehl, 1980) and the Dakota aquifer in South Dakota (Bredehoeft, Neuzil, and Milly, 1983), both first exploited in the 1880s, offer well-known instances where high fluid pressures are due to the presence of low-permeability argillaceous confining layers. Some sense of the hydraulics of this type of flow regime can be gotten from figure 1, a simplified depiction of the Great Artesian Basin. The energy

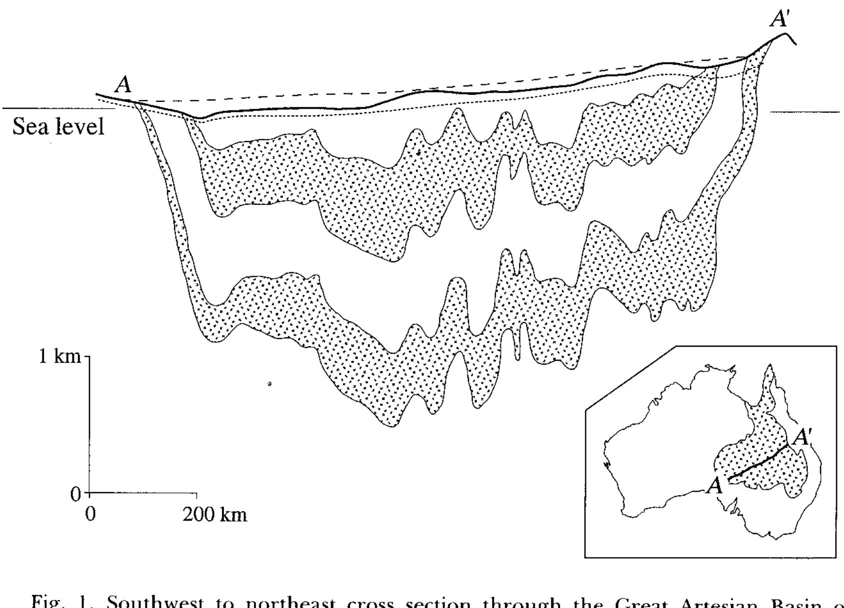

Fig. 1. Southwest to northeast cross section through the Great Artesian Basin of Australia showing abnormally high fluid pressures. The stipple pattern shows permeable (aquifer) units, the dotted line shows the elevation of the water table, and the dashed line shows hydraulic heads in the lower (Jurassic) permeable unit in 1880. The slope of the dashed line represents the energy dissipated by flow (adapted from Habermehl, 1980, fig. 18).

that generates the high pressures and drives the flow is derived from the high elevation of the groundwater recharge in the northeast, where the aquifers crop out.

Topographically-driven flow is also capable of producing quite pronounced abnormally low pressures. The Denver Basin provides a striking example, with Cretaceous sandstones displaying hydraulic heads as much as 900 m below land surface, as shown in figure 2. Belitz and Bredehoeft (1988) have demonstrated that the low pressures are readily explained as occurring in an equilibrated flow system governed by (12). Their conceptual model of the system invokes a basin structure in which faults along the Rocky Mountain front (at B in fig. 2) and low-permeability shale limit recharge to the permeable sandstones, which nevertheless discharge readily at low elevation outcrops in the east (at B′). In effect, they see the sandstones as a regional drain, lowering heads in the center of the basin. Groundwater recharge at high topographic elevations cannot raise the heads in the system because of the large energy losses incurred during downward flow across the shale (fig. 2).

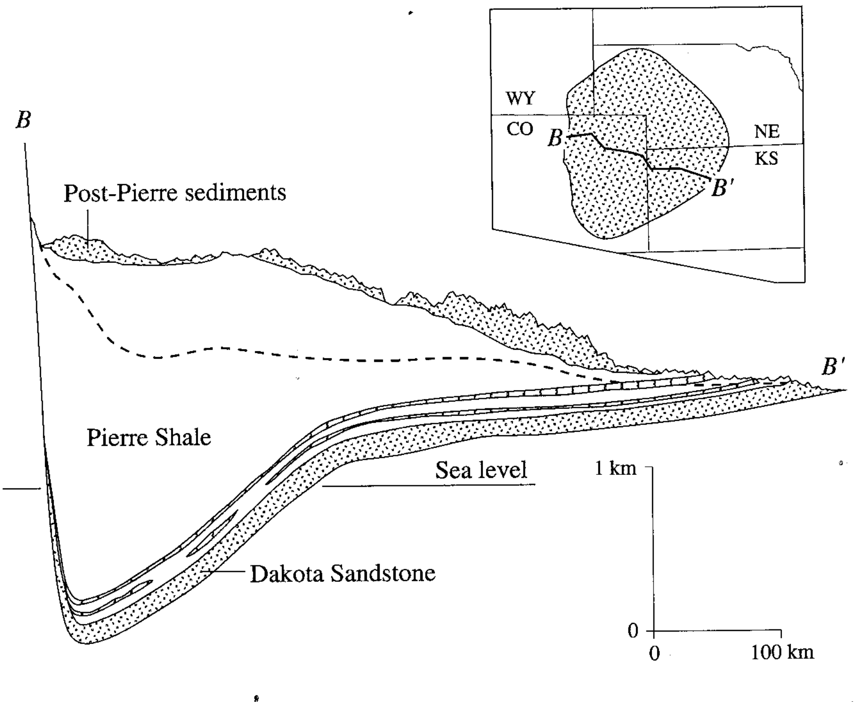

Fig. 2. West to east cross section through the Denver Basin, Western Interior North America, showing abnormally low fluid pressures. The stipple and block patterns indicate permeable arenaceous and carbonate units (aquifers). The dashed line is the hydraulic head in the Dakota Sandstone; the water-table is too close to the land surface to be shown. The cross section was constructed using information from the Petroleum Information Corporation and other sources.

Chemically-driven Flow

There are relatively few flow systems thought to be driven osmotically by chemical potential gradients. Examples include portions of the San Juan Basin in Utah, Colorado, and New Mexico (Berry, 1959; Hanshaw and Hill, 1969), portions of the San Joaquin Valley, California (Berry and Hanshaw, 1960), the Gulf Coast (Magara, 1974), and the Triassic Dunbarton Basin in South Carolina and Georgia (Marine and Fritz, 1981). Invariably, attribution of abnormal pressures to osmosis has proven controversial (Neuzil, 1986). Nevertheless, it is clear that argillaceous media can act as osmotic membranes (Olsen, 1972; Neuzil, unpublished data); flow driven by chemical potential gradients is a possibility when salinity gradients and argillaceous rocks are present. Specifically, osmotically-driven flow cannot be ruled out when abnormally high fluid pressures coincide with regions of comparatively high salinity or abnormally low fluid pressures coincide with regions of comparatively low salinity.

Osmotically-driven systems become hydrodynamically equilibrated relatively quickly even though diffusion and advection alter the salinity distribution over long periods of time (Mitchell, Greenberg, and Witherspoon, 1973). In effect, the slowly changing salinity distribution can be considered an aspect of the evolving geologic framework; the flow regime remains adjusted to it. Interestingly, this exceptional type of abnormally pressured system occurs without fluid flow. The absence of flow represents a hydrodynamic stasis, with chemical driving forces balanced by opposing hydraulic driving forces. The nature of this balance becomes apparent when (11) is rewritten as

$$\nabla \cdot \kappa \nabla h = \nabla \cdot \frac{\kappa_c}{c} \nabla c. \tag{13}$$

As (13) makes clear, a pressure perturbation marked by a nonzero ∇h must be present when κ_c and ∇c are nonzero.

Marine and Fritz (1981) have described one of the best documented examples of abnormal pressure attributed to chemical osmosis (fig. 3). Hydraulic heads approx 130 m above hydrostatic occur in Triassic sediments, coinciding with salinities of 12,000 to 19,000 mg/l. The surrounding, normally-pressured crystalline rocks and overlying coastal plain sediments have salinities less than 6000 mg/l. As figure 3 shows, there is a good correspondence between high salinity and high fluid pressures. Theoretical calculations of κ_c by Marine and Fritz (1981) led them to conclude that osmosis could have generated the high pressures. This claim of osmotic pressuring is particularly noteworthy because Marine and Fritz (1981) carefully considered and ruled out alternative causes of the pressures.

Density Contrasts and Non-water Phases

Abnormal pressures also occur in the absence of flow as a result of pore fluid heterogeneity. Density contrasts because of differences in

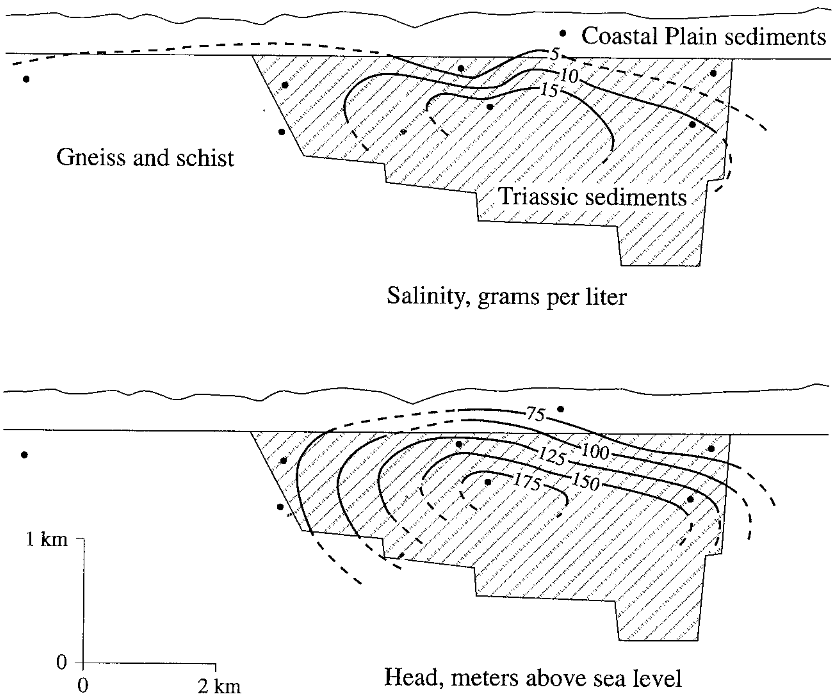

Fig. 3 Northwest to southeast cross sections through the Dunbarton Basin, South Carolina and Georgia, showing abnormally high pressures thought to be generated by osmosis. The cross sections were constructed using data published by Marine and Fritz (1981).

salinity or, to a greater degree, because of distinct phases such as petroleum, natural gas, or carbon dioxide give rise to abnormal pressures as hydrostatic phenomena, representing a special type of equilibrated system. For example, a rock section containing brine will have pressures in excess of fresh water hydrostatic. Usually, however, full abnormal pressures are produced only by accumulations of petroleum or natural gas. The abnormal pressures occur in geologic structures of significant vertical extent where hydrocarbons are trapped by capillary forces. In structures trapping gas, the pressure throughout the accumulation is essentially the same as that of the underlying liquid phase. If the gas accumulation is sufficiently thick, its pressure in the upper portions of the structure will be abnormally high.

A clearly delineated example of abnormally high pressures due to fluid heterogeneity was described by Dickinson (1953) and is shown in figure 4. The high pressures occur in a Gulf Coast sand unit upwarped along the flank of a salt dome and containing water, petroleum, and

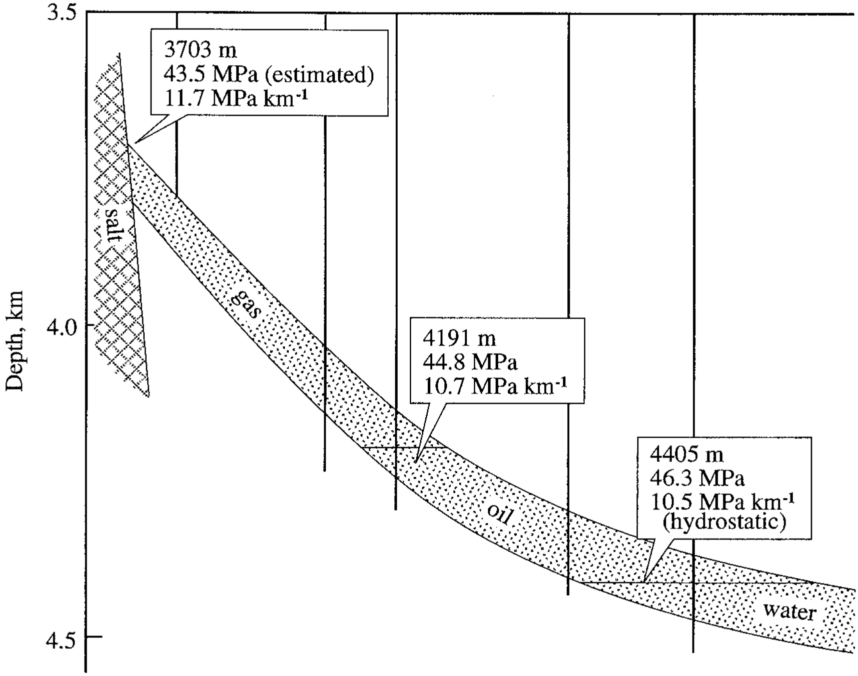

Fig. 4. Cross section of the "S" Sand unit in the Louisiana Gulf Coast, showing the disposition of gas, oil, and water as well as pressures and pressure gradients at selected levels. Vertical lines are boreholes (depiction based on Dickinson, 1953, fig. 12, and Fertl, 1976, fig. 1.14).

natural gas. Pressures in the water are normal, or hydrostatic, but depart from hydrostatic with elevation in the hydrocarbon column.

Many abnormal pressure data come from hydrocarbon provinces and reflect the presence of hydrocarbon phases that are less dense than water. However, as I stated earlier, the overpressuring due to distinct fluid phases typically does not account for these abnormal pressures. In the Gulf Coast sand reservoir depicted in figure 4, for example, the maximum pressure gradient is 11.8 MPa km^{-1}, slightly over the normal pressure gradient in this area of 10.5 MPa km^{-1} (Dickinson, 1953). This represents a small fraction of the very strong overpressuring, with gradients reaching 20 MPa km^{-1}, that is found in the Gulf Coast (Kreitler and others, 1988). Similar relationships have been described in other oil and gas regions. Hubbert and Rubey (1959) showed that less than 10 percent of the high pressure in the Qum, Agha Jari, and Naft Safid oil fields in Iran is attributable to density effects. Likewise, significant accumulations of oil and gas are present in Rocky Mountain basins discussed by Spencer (1987), but, according to him, density effects account for only local pressure perturbations in these regionally overpressured systems.

ABNORMAL PRESSURES AS NATURAL DISEQUILIBRIA

The systems discussed thus far are examples of equilibrium hydrodynamics (including hydrostatics as a special case). However, most abnormal pressures are not easily explained by equilibrium hydrodynamics. For example, high pressures are found in coastal and offshore areas where nearby topography, chemical potential gradients, and density contrasts are insufficient to account for the pressure. It is also apparent that certain abnormal pressures are isolated in three dimensions as discrete regions of high or low hydraulic head. Both circumstances are hallmarks of natural hydrodynamic disequilibrium. Disequilibrium results from the tendency for changes in both the fluid pressure and the geologic setting itself to push flow regimes away from an equilibrated, topographically- or chemically-driven state. Heuristically, a disequilibrium flow regime may be described as one that was unable to evolve rapidly enough to accommodate the natural changes imposed upon it. Disequilibrium cannot be understood in the context of the current state of the system alone; the system's history must also be taken into account.

Generation of Disequilibrium-type Abnormal Pressures

Fluid throughflow occurs in equilibrated, topographically-driven regimes because the highest and lowest hydraulic heads occur at the system boundaries. Disequilibrium represents a disruption of this pattern; often, the highest or lowest head occurs *within* the system, and there is a resulting net flux of fluid in or out. This is a direct consequence of Γ in the role of a distributed source or sink. Ideal disequilibrium head patterns in a homogeneous stratum of rock are presented in figure 5.

Under what conditions should disequilibrium-type abnormal pressures be expected? In order to address this question it is convenient to use a nondimensionalized form of (9), namely

$$\nabla_D^2 h_D = \frac{\partial h_D}{\partial t_D} + \Gamma_D \tag{14}$$

where ∇_D^2 and h_D are the Laplacian operator and hydraulic head nondimensionalized with a representative length l, dimensionless time $t_D = \kappa t/S_s' l^2$, dimensionless geologic forcing $\Gamma_D = (l/\kappa)\Gamma$, and it has been assumed that chemical driving forces can be ignored. I define l as the characteristic flow length of a domain, equal to the distance from the domain center to its nearest boundary; $2l$ thus approximates the smallest dimension of the domain (fig. 5).

Of interest are conditions where disequilibrium becomes sufficiently pronounced to cause abnormal pressures. The degree of disequilibrium can be characterized nondimensionally by the hydraulic head gradients it creates; in a domain with l on the order of 10^2 m, hydraulic gradients of unity or greater indicate abnormal pressure as defined in this paper, that is, pressure differing from hydrostatic by 100 m of hydraulic head (this should be apparent from fig. 5). In larger domains, unit gradients

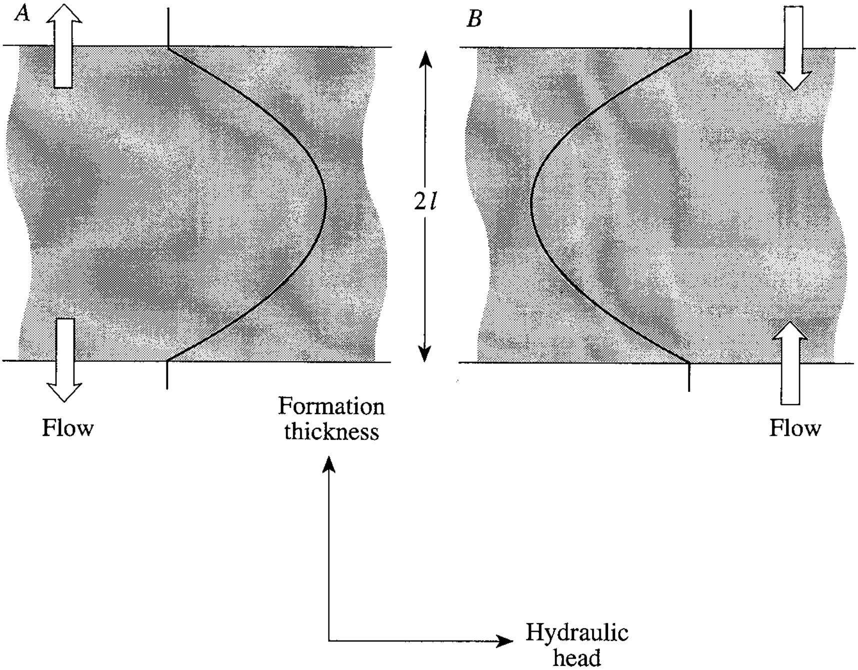

Fig. 5. Hydrodynamic disequilibrium caused by geologic forcing in a homogeneous low-permeability layer between permeable strata with normal pressures. (A) negative Γ: fluid pressures and hydraulic heads increase, causing outward flow. (B) positive Γ: fluid pressures and hydraulic heads decrease, causing inward flow. In actual subsurface environments, these patterns are superimposed on any topographically- or chemically-driven flow that may be present.

indicate even more pronounced nonhydrostatic pressures. A conservative and broadly applicable criterion for abnormal pressures is therefore one that results in disequilibrium hydraulic gradients of unity. As it turns out, such a criterion can be stated quite simply. Solutions of (14) for a variety of domain geometries (for example Carslaw and Jaeger, 1959, p. 130) indicate that gradients on the order of unity or larger are generated when $|\Gamma_D| > 1$, or

$$|\Gamma| > \kappa/l. \tag{15}$$

This inequality is a quite general, if approximate, indicator of conditions leading to disequilibrium-type abnormal pressures. It formally demonstrates that disequilibrium-type abnormal pressures are favored by low permeability, a fact implicitly recognized for some time. It also shows that the size of the domain and the strength of the geologic forcing are equally important.

Low permeability in the crust.—Certain types of sedimentary units and some crystalline rock masses appear to have quite low permeabilities.

Elsewhere (Neuzil, 1994), I presented data indicating that argillaceous sediments often have largely scale-independent permeabilities between 10^{-22} and 10^{-17} m^2 (roughly equivalent to κ between 10^{-15} and 10^{-10} ms^{-1}) that are governed mainly by the degree of compaction. An earlier compilation by Brace (1980) had suggested largely scale-independent permeabilities as low as 10^{-21} m^2 for argillaceous rocks. Evaporites, including halite, appear to have a similar range of permeabilities (Bredehoeft, 1988; Beauheim and others, 1991), although pure halite seems to have an exceptionally small permeability that is less than 10^{-22} m^2 (R. Beauheim, Sandia National Laboratory, personal communication, 1994).

Sedimentary media that typically have relatively large permeabilities, such as arenaceous rocks, may themselves contain zones of quite low permeability. These zones, often referred to as seals, frequently are described as nearly horizontal and cutting across stratigraphic horizons (Hunt, 1990; Powley, 1990), suggesting a tie to at least partly temperature controlled diagenetic processes. However, Hunt (1990) and Powley (1990) also described nonhorizontal seals that act as lateral flow barriers and, together with horizontal seals, compartmentalize portions of the subsurface. Moline and others (1992) ascribed low permeability zones in the St. Peter Sandstone of the Michigan Basin to secondary cementing by quartz and dolomite, while Weedman, Guber, and Engelder (1992) hypothesized that a similar feature in the Tuscaloosa Formation in Louisiana formed after quartz dissolution led to secondary compaction. There are few permeability data for these features; results obtained by Moline and others (1992) suggest values on the order of 10^{-18} to 10^{-17} m^2 (10^{-11}-10^{-10} ms^{-1}) or less for low-permeability zones in the St. Peter Sandstone.

Relatively large permeabilities are generally thought to apply in crystalline rock at the scales of interest ($l > 10^2$ m) because of ubiquitous fracturing (Brace, 1980). Nevertheless, there is some reason to believe that connected fracture permeability is not always present in crystalline rocks, especially at depths of 7 to 12 km or more where some plastic deformation may occur (Walder and Nur, 1984). Experiments conducted by Trimmer and others (1980) yielded permeabilities for unfractured crystalline rock that are quite low, between 10^{-24} and 10^{-20} m^2 (κ between 10^{-17} and 10^{-13} ms^{-1}). Walder and Nur (1984) suggested somewhat higher values of 10^{-20} to 10^{-19} m^2 for rocks at depths of 7 to 12 km.

Of course, the concept of a single "permeability" for large volumes of sediment or rock ignores many of the complexities of geologic environments. Consideration of this problem is deferred to a later section where the relation between permeability and abnormal pressure is considered in more detail.

Strength of geologic forcing.—Based on the preceding discussion we may expect to encounter large regions ($l > 10^2$ m) composed of or bounded by media with permeabilities between 10^{-22} and 10^{-17} m^2 (κ between 10^{-15}-10^{-10} ms^{-1}). Inequality (15) indicates that when permeability is in this range, forcing between 10^{-17} and 10^{-12} s^{-1} is significant (that is, able to maintain abnormal pressures). Similarly, forcing between 10^{-18} and 10^{-13} s^{-1} is significant in domains where l is on the order of 1 km.

One might expect the magnitude of Γ to be difficult to characterize because forcing is a complex phenomenon arising from many different geologic processes. While it is true that evaluating forcing in specific situations is often problematic, estimated ranges of Γ values associated with many different processes can be obtained from the literature without great difficulty; these are listed in table 1. An intriguing conclusion that can be drawn from table 1 is that a host of quite distinct processes cause significant geologic forcing. Indeed, to a surprising degree, the magnitudes of various kinds of forcing are comparable, falling between 10^{-15} s^{-1} and 10^{-13} s^{-1}. On the strength of this observation, hydrodynamic disequilibrium seems to be a viable model for abnormal pressures in a wide variety of geologic settings.

Active Versus Remnant Disequilibrium

Disequilibrium does not result solely from active forcing as represented by Γ in (9) and (14). In principle, changes in boundary conditions can also generate disequilibrium. This might occur, for example, when erosion exposes a new recharge or discharge area for an aquifer, or faulting changes a permeability pattern. Instances of this are rare at best, and I am aware of no well-documented examples. Alternatively, it is possible for a disequilibrium regime that we detect today to be a decaying remnant of a once geologically active system forced by processes that are no longer active. Hydrodynamically, the two possibilities are indistinguishable. In either case, the disequilibrium decays in a manner described by (9) or (14) when Γ is set to zero, and the initial condition describes the state of disequilibrium. Used in this way, the equation describes the return to equilibrium, usually topographically-driven flow. Solutions of (14) for this problem, which are well known from analogous problems in other disciplines (for example, Šuklje, 1969, p. 139), show that abnormal pressures would begin to suffer significant dissipation after $t_D \approx 0.1$ or $t \approx 0.1\ (S'_s l^2)/\kappa$; for reasonable dimensions and permeabilities, such as those of the system analyzed by Tóth and Millar (1983); this is on the order of 10^5 yrs.

Most abnormal pressures are thought to be much older than 10^5 yrs. One can readily find instances where disequilibrium has apparently persisted for 10^7 yrs or longer, such as the western Canada sedimentary basin (Corbet and Bethke, 1992) and the U.S. Gulf Coast (Harrison and Summa, 1991). By comparison, observing a disequilibrium system as it decays to an equilibrium state would imply rather lucky timing. We may infer that the vast majority of disequilibrium abnormal pressures owe their existence to ongoing forcing and can be characterized in terms of inequality (15). By extension, a key characteristic of most disequilibrium-type abnormal pressures is a dynamic balance between processes tending to create abnormal pressures and the resulting flow, which tends to

TABLE 1

Geologic forcing in various settings

Environment or Process	Γ	Magnitude (s^{-1})	Comments	Sources
UPPER CRUST				
Subsidence and sedimentation				
Compaction and heating	$-\zeta_m \frac{\partial \sigma_t}{\partial t} - \zeta_T \frac{\partial T}{\partial t} = -\left[\frac{1+\nu}{3(1-\nu)}\zeta_m \gamma' + \zeta_T G\right]\frac{\partial L}{\partial t}$	up to 7×10^{-15}	Caused by increasing weight of overburden and displacement through geothermal gradient. Maximum value assumes $\zeta_m = 10^{-8}$ Pa^{-1}, $\zeta_T = 10^{-4}\ °C^{-1}$, a geothermal gradient G of 60°C km^{-1}, a sedimentation rate, $\partial L/\partial t$, of 10^2 cm kyr^{-1}, a specific weight of saturated sediment γ' of 2.3×10^4 kg m^{-2} s^{-2}, and a Poisson's ratio ν of 0.25.	Domenico and Palciauskas (1979); Bethke (1986)
Dewatering of smectitic clay	$\left(\frac{\partial n}{\partial t}\right)^* - J/\rho = (B-1)(1-n)\frac{dX}{dz}v_z$	up to 3×10^{-15}	B is volume of free water produced by release of unit volume of hydrated water, X is ratio of volume of structural water to dehydrated mineral, and v_z is the burial rate. Maximum value assumes $B = 1.4$, $n = 0.3$, $dX/dz = 3.6 \times 10^{-4}\ m^{-1}$ and $v_z = 10^2$ cm kyr^{-1}.	Bethke (1986)
Uplift and erosion				
Decompaction and cooling	$-\zeta_m \frac{\partial \sigma_t}{\partial t} - \zeta_T \frac{\partial T}{\partial t} = -\left[\frac{1+\nu}{3(1-\nu)}\zeta_m \gamma' + \zeta_T G\right]\frac{\partial L}{\partial t}$	up to 7×10^{-15}	Caused by decreasing weight of overburden and displacement through geothermal gradient. Maximum value assumes $\zeta_m = 10^{-8}$ Pa^{-1}, $\zeta_T = 10^{-4}\ °C^{-1}$, a geothermal gradient G of 60°C km^{-1}, an erosion rate, $-\partial L/\partial t$, of 10^2 cm kyr^{-1}, a specific weight of saturated sediment γ' of 2.3×10^4 kg m^{-2} s^{-2}, and a Poisson's ratio ν of 0.25.	Neuzil and Pollock (1983); Neuzil (1993)
Other				
Petroleum generation	$\left(\frac{\partial n}{\partial t}\right)^* - J/\rho = -\frac{\rho_k - \rho_p}{\rho_p}kV$	up to 1×10^{-14}	V is volume of kerogen per volume of rock, ρ_k is kerogen density, ρ_p is petroleum density, and k is the rate constant for the petroleum generation. Maximum value assumes $V = 0.3$, $k = 3 \times 10^{-13}\ s^{-1}$, $\rho_k = 1.05$ gm cm^{-3}, and $\rho_p = 0.95$ gm cm^{-3}.	Bredehoeft, Wesley, and Fouch (1994)

Pressure solution	$\left(\frac{\partial n}{\partial t}\right)^* = -\alpha_i \frac{\partial \sigma_v}{\partial t}$	up to 4×10^{-15}	α_i is inelastic "compressibility". Maximum value assumes $\alpha_i = 5 \times 10^{-9}\ Pa^{-1}$, and a burial rate of 10^2 cm kyr^{-1}.	Palciauskas and Domenico (1989)
	$\left(\frac{\partial n}{\partial t}\right)^* = f\left(\frac{\partial \sigma'}{\partial t}, \frac{\partial T}{\partial t}\right)$	up to 10^{-15}	Maximum value assumed burial at 10^2 cm kyr^{-1} and G = 27°C km^{-1}	Stephenson, Plumley, and Palciauskas (1992)
	$\left(\frac{\partial n}{\partial t}\right)^* = f(\sigma', C_q, \rho_q, d, D)$	10^{-16} to 10^{-15}	For quartz sand, σ' is effective stress, C_q is equilibrium concentration of quartz in pore fluid, ρ_q is density of quartz, d is grain diameter, and D is rate of diffusion in grain to grain contact.	Angevine and Turcotte (1993)
	$\left(\frac{\partial n}{\partial t}\right)^* = f(\sigma', C_q, \rho_q, d, D)$	up to 10^{-14}	Maximum value is for quartz sand at 300°C.	Gratz (1991)
Microbial processes	$\left(\frac{\partial n}{\partial t}\right)^* = f(T, \text{chemistry})$	more than 5×10^{-17}	For quartz sand. Limited to temperatures below 100°C.	McMahon and others (1992)
Crustal deformation				
Stable intraplate and passive margin	$-\zeta_m \frac{\partial \sigma_t}{\partial t} = -\xi\dot{\epsilon}$	10^{-23} to 10^{-20}	Assumes $\xi = 0.1$ and ratio of volumetric strain to linear surface deformation of 0.1	Anderson (1986)
Active intraplate	$-\zeta_m \frac{\partial \sigma_t}{\partial t} = -\xi\dot{\epsilon}$	10^{-20} to 10^{-18}	Assumes $\xi = 0.1$ and ratio of volumetric strain to linear surface deformation of 0.1	Anderson (1986)
Vicinity of transform fault	$-\zeta_m \frac{\partial \sigma_t}{\partial t} = -\xi\dot{\epsilon}$	2×10^{-15}	Assumes $\xi = 0.1$ and ratio of volumetric strain to linear surface deformation of 0.1	Pfiffner and Ramsay (1982)
Orogenic zones	$-\zeta_m \frac{\partial \sigma_t}{\partial t} = -\xi\dot{\epsilon}$	10^{-17} to 10^{-15}	Assumes $\xi = 0.1$ and ratio of volumetric strain to linear surface deformation of 0.1	Pfiffner and Ramsay (1982)
Accretionary prism	$-\zeta_m \frac{\partial \sigma_t}{\partial t} = -\xi\dot{\epsilon}$	10^{-15} to 10^{-13}	Computed porosity loss during accretion based on convergence rate.	Screaton, Wuthrich, and Dreiss (1990)

TABLE 1
(continued)

Environment or Process	Γ	Magnitude (s^{-1})	Comments	Sources
MID CRUST				
Regional metamorphism				
Fluid generation by devolatilization	$\frac{J}{\rho}$	up to 2×10^{-15}	Metamorphism of 10 km of pelitic rock over 4.3 Ma. Assumes density of volatiles is 500 $kg\ m^{-3}$	Walther and Orville (1982)
	$\frac{J}{\rho} = \frac{X_f R}{\Delta T_r} \frac{\partial T}{\partial t}$	up to 3×10^{-15}	X_f is weight fraction of fluid in rock released over temperature interval ΔT_r. R is ratio of solid density to fluid density. Maximum value assumes $X_f = 0.05$, $R = 5.5$, $\Delta T_r = 300°C$ and $\partial T/\partial t = 3 \times 10^{-12}\ °C\ s^{-1}$.	Hanson (1992)
Inelastic deformation	$\left(\frac{\partial n}{\partial t}\right)^*$	10^{-16} to 10^{-15}	Mechanism unclear; possibly plastic deformation of grains or pressure solution	Walder and Nur (1984)
Contact metamorphism				
Fluid generation by devolatilization	$\frac{J}{\rho} = \frac{X_f R}{\Delta T_r} \frac{\partial T}{\partial t}$	3×10^{-13}(?)	X_f is weight fraction of fluid in rock released over temperature interval ΔT_r. R is ratio of solid density to fluid density. Assumes $X_f = 0.05$, $R = 5.5$, $\Delta T_r = 300°C$ and $\partial T/\partial t = 3 \times 10^{-9}\ °C\ s^{-1}$.	Hanson (1992)
Heating of fluid and porous matrix	$-\zeta_T \frac{\partial T}{\partial t}$	3×10^{-13}	Assumes $\zeta_T = 10^{-4}\ °C^{-1}$ and $\partial T/\partial t = 3 \times 10^{-9}\ °C\ s^{-1}$.	Palciauskas and Domenico (1982)

dissipate it. The balance is not a stasis but must continually shift because domain geometries, rock hydraulic properties, and the forcing itself vary in time. Often, this inherently transient nature is not associated with abnormal pressures because the changes are far too gradual to detect.

Implications of the Disequilibrium Model

The relationship represented by (15) implies that different disequilibrium-type abnormal pressure regimes can be compared in terms of the magnitude of the forcing and the permeability and dimensions of their domains. Figure 6 makes this comparison among several abnormal pressure regimes for which the relevant properties are known or have been estimated. There is commonly uncertainty, sometimes significant, in the magnitude of forcing and the permeability of specific systems, a fact reflected in the size of the plotted regions in figure 6. The plot suggests that the forcing in these abnormal pressure environments ranges between 10^{-19} and 10^{-13} s^{-1}, with a similar order-of-magnitude range in κ. Fluid pressures in more permeable media can be similarly affected by highly intense forcing such as aseismic creep along active faults (Byerlee, 1993) and heating caused by igneous intrusive activity (Norton, 1990). Such phenomena could also be represented on figure 6 but would plot beyond the right-hand boundary. They are not an important consideration here, because the pressure perturbations tend to be comparatively short-lived and localized.

It is possible for the criterion expressed by (15) to be exceeded by a significant margin. Indeed, this possibility is clear from the range of forcing, permeability, and dimensions evident in figure 6. In such instances, forcing could drive pressures above lithostatic or below atmo-

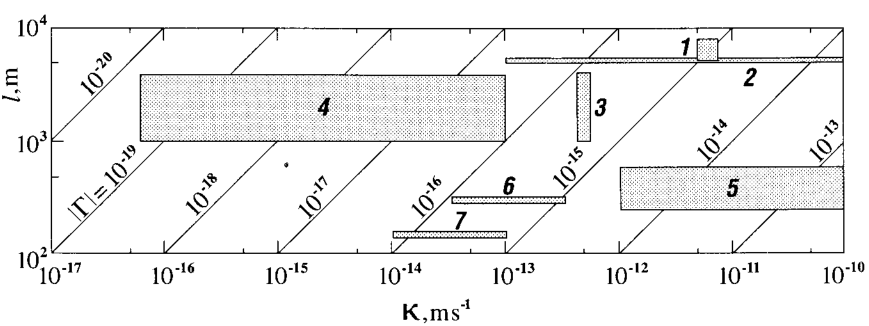

Fig. 6. Plot of the relation $|\Gamma| = \kappa/l$ allowing comparison of a variety of disequilibrium-type abnormal pressure regimes. The regions shown represent: (1) Franciscan sediments, California (Berry, 1973; Unruh and others, 1992); (2) U.S. Gulf Coast (Harrison and Summa, 1991); (3) high fluid pressures at 7 to 12 km depth in various locations (Walder and Nur, 1984); (4) alternate interpretation of region 3 using permeability of unfractured crystalline rock measured by Trimmer and others (1980); (5) Barbados accretionary complex (Screaton, Wuthrich, and Dreiss, 1990); (6) western Canada sedimentary basin (Corbet and Bethke, 1992); (7) Pierre Shale in South Dakota (Neuzil, 1993).

spheric and into the negative range. If fluid pressure exceeds lithostatic (or more accurately the least principal stress, which is usually similar) dilatation and natural hydrofracturing may occur. The dilatation and fracturing accommodate the fluid, and if interconnected fractures are formed, they relieve the high pressure by significantly increasing the permeability. Researchers have found direct evidence of this process in Gulf Coast shale (Capuano, 1993) and have speculated that it occurs in crystalline rock (Walder and Nur, 1984). At the other extreme, as fluid pressure drops, two things can happen: pressure can continue to decrease to negative absolute values (Tóth, 1981; Neuzil and Pollock, 1983) or a vapor phase can form by cavitation (Neuzil and Pollock, 1983). Subsurface pressures below zero absolute have not been reported, possibly because detecting them would be difficult. Regimes in which they may have occurred have been identified by Tóth (1981) and Neuzil (1993).

Disequilibrium domains are not fully isolated from their surroundings; as noted previously and shown schematically in figure 5, there is inward or outward flow across the domain boundaries. However, the fluxes involved are quite small and influence only regions near the boundaries. Disequilibrium domains must, in fact, sequester water and solutes quite effectively for long periods of time. This can easily be seen by considering, as a hypothetical example, an extensive kilometer-thick stratum hosting disequilibrium-type abnormal pressure. Even assuming that the disequilibrium is caused by a relatively vigorous forcing of 10^{-14} s^{-1}, this only amounts to a virtual source or sink throughout the stratum of 10^{-11} m^3 s^{-1} per m^2 of area. Flow across the boundaries must be less than this, or abnormal pressures would not exist. Thus the Darcy flux across each boundary would be less than 5×10^{-12} ms^{-1}. For a representative porosity of 0.3, this amounts to a transport distance of less than 50 m in 10^5 yrs. This rate of fluid transport is comparable to that of diffusive solute transport in porous media. Indeed, the loss or gain of chemical mass to these environments and their chemical evolution is controlled by diffusion.

Occurrence of Disequilibrium-Type Abnormal Pressure

Table 1 suggests that opportunities for generating disequilibrium-type abnormal pressures are abundant and varied in the dynamic crust. This section examines a few selected examples of abnormal pressures that have been interpreted as disequilibrium regimes and considers the nature of the geologic forcing thought to have produced them. The selection is not intended to be comprehensive. Rather, I have chosen examples that seem to be reasonably well understood or that help to demonstrate the diversity of disequilibrium-type abnormal pressure regimes in nature. They are considered in the context of major types of geologic environments in the upper crust.

Active sedimentary basins.—Prolonged crustal subsidence and active sedimentation are occurring in many locales worldwide, particularly where major river systems disgorge. Prominent examples include the

U.S. Gulf Coast, the Niger delta, the Caspian basin, the Indus delta, and the Orinoco delta. Subsidence and sedimentation in these environments drive several processes that can generate disequilibrium. The accumulation of sediment adds ever increasing overburden loads on the underlying sediments which are also heated as they are displaced downward through the geothermal gradient (Domenico and Palciauskas, 1979). A reasonable approximation of the forcing due to the linked processes of loading and heating can be expressed as

$$\Gamma = -\zeta_m \frac{\partial \sigma_t}{\partial t} - \zeta_\Gamma \frac{\partial T}{\partial t} = f(R_d). \tag{16}$$

These processes depend almost exclusively on R_d, the deposition rate. Although burial also causes diagenesis, diagenetic effects are not included in (16) to emphasize that they are not simply related to R_d. Instead, processes such as pressure solution (Palciauskas and Domenico, 1989; Gratz, 1991; Oelkers, Bjorkum, and Murphy, 1992; Stephenson, Plumley, and Palciauskas, 1992), smectite dewatering (Bethke, 1986), and microbially mediated porosity loss (McMahon and others, 1992), are controlled in a complex manner by several environmental factors and can be represented as

$$\Gamma = \left(\frac{\partial n}{\partial t}\right)^* - \frac{J}{\rho} = f(T, P, \sigma_t, t). \tag{17}$$

For completeness, we must also look beyond the upper 10 km or so of sediment usually considered; deeper sediments, largely beyond the reach of drilling, also experience increasing temperatures and stresses. At these depths, between perhaps 10 and 20 km, porosity is low and compaction due to increasing load σ_t in (16) probably no longer produces significant forcing. However, thermomechanical effects represented in (16) and diagenesis/metamorphism represented in (17) could be significant. In particular, sediments will be devolatilized at high temperatures as metamorphism begins. The resulting forcing is largely dependent on the rate of heating (Walther and Orville, 1982; Hanson, 1992; table 1) and thus mainly dependent on R_d.

The U.S. Gulf Coast is probably the most studied active basin environment with abnormal pressures and displays most, if not all, the types of forcing found in these environments. The fluid pressures there often approach lithostatic; they are associated with shale-rich sequences and generally are separated from superposed hydrostatically pressured sediments by steep hydraulic gradients. Figure 7, which shows results of simulations of Gulf Coast abnormal pressures obtained by Bethke (1989), gives some impression of their large dimensions and one interpretation of their development and longevity.

Numerous other researchers, exemplified by Bredehoeft and Hanshaw (1968), Domenico and Palciauskas (1979), and Harrison and Summa (1991) have also analyzed the high fluid pressures in the Gulf Coast as

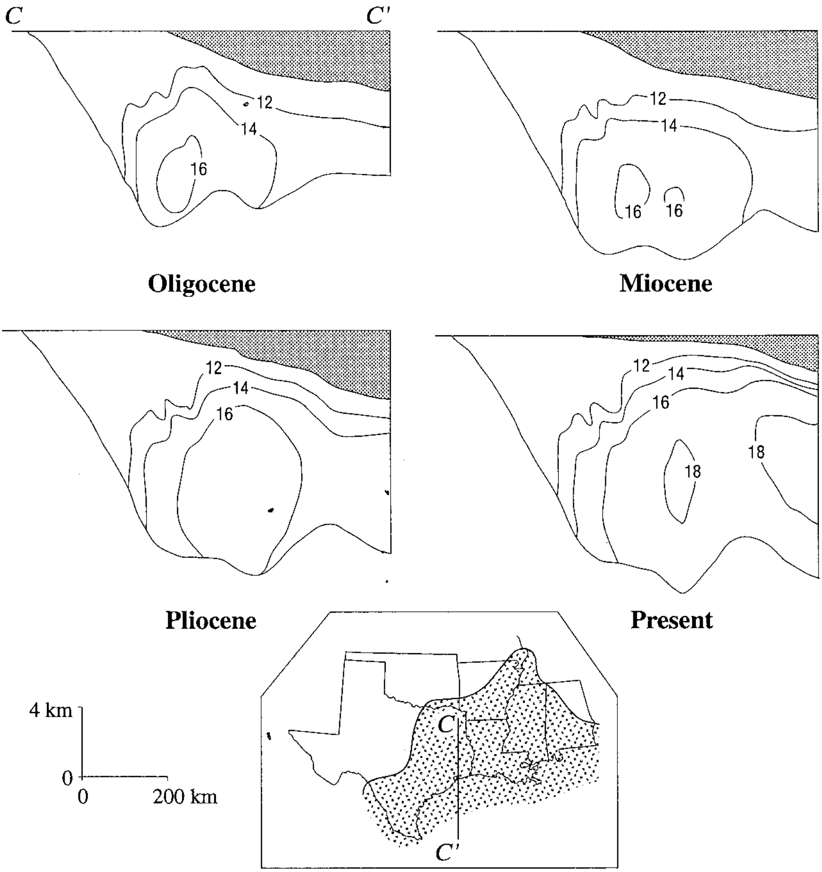

Fig. 7. Disequilibrium-type abnormal pressure regime in a vertical slice through the U.S. Gulf Coast as simulated by Bethke (1989). Contoured values are pressure gradients with depth relative to the surface in MPa km^{-1}; hydrostatic gradients are between 9.7 and 11.3 MPa km^{-1} depending on the salinity of the pore fluid. Oligocene, Miocene, and Pliocene sections represent conditions 31, 5.2, and 1.8 Ma before present, respectively (adapted from Bethke, 1989, fig. 5).

hydrodynamic disequilibria. There is little difficulty identifying several forms of geologic forcing in the Gulf Coast, where sediments are accumulating as rapidly as 5 m per thousand yrs. The studies mentioned above, as well as several others, indicate that compactional porosity loss alone (represented by the first term in (16)) is sufficient to cause the high pressures, with second-order effects from thermal expansion (the second term in (16); see table 1). Work by Bethke (1986) suggests that diagenetic fluid sources and porosity changes described by (17) may also have played an important role (table 1). According to Bethke (1986), interlayer water is expelled from smectite, and the clay experiences a volume decrease which effectively increases the porosity. However, the water experiences a decrease in density upon expulsion, tending to increase fluid pressure; in other words, both $(\partial n/\partial t)^*$ and J/ρ in (17) are nonzero and positive, but the latter is larger.

The history of Gulf Coast geopressures, as depicted in figure 7, nicely illustrates both the balance between forcing and flow in disequilibrium regimes and the tendency for disequilibrium systems to change through time. The simulations suggest that in Miocene time, geopressure gradients up to 16 MPa km^{-1} were present beneath the loci of deposition. When deposition accelerated and shifted seaward in late Miocene to early Pliocene, geopressures probably became more extensive and pronounced, with gradients exceeding 18 MPa km^{-1}, and also migrated seaward (fig. 7). The change in the pattern and intensity of geopressures was also brought about, in part, by changing domain geometry (thickening through deposition) and decreasing permeability brought about by compaction.

Investigators who have analyzed the Gulf Coast have typically considered only the upper 10 km, more or less, of sediment. Deeper sediments and underlying basement rock are not explicitly included in simulations of abnormal pressure development; it is generally assumed that the simulation domain has an impermeable lower boundary. In Bethke's (1989) simulations (fig. 7) the impermeable bottom boundary represented the Louann Salt, which may in fact be essentially impermeable. Nevertheless, high fluid pressures could exist at greater depths due to diagenesis and metamorphism of the pre-Louann sediments. They might even contribute directly to the abnormal pressures observed at lesser depths.

Ancient sedimentary basins.—In comparison with active sedimentary basins, a more diverse and arguably more complex suite of abnormal pressures is encountered in sedimentary sequences that have experienced quiescence and, in some cases, uplift, erosion, and deformation. Abnormal pressures are well known from the Anadarko and Delaware Basins (Fertl, 1976), the Appalachian region (Russell, 1972), the western Canada basin (Hitchon, 1969b), several Rocky Mountain Basins (Spencer, 1987) as well as old sedimentary terrains in Europe, Africa, and Asia (Hunt, 1990). Unlike active basins, ancient basins frequently host pressures that are abnormally low as well as abnormally high, occasionally comingling the two as is seen in the Anadarko Basin.

Forcing in these environments may be less obvious than in subsiding basins, although they in fact host a widely varied suite of processes that can affect fluid pressure. Much of the forcing is still described by (16) and (17). Unlike active basins, however, the derivatives in (16), in this case a function of the erosion rate, have negative values and tend to lower fluid pressure, offering an explanation for abnormally low pressures. However, certain diagenetic processes represented by (17) may still act to increase pressure. For example, porosity loss by pressure solution may continue at depths less than the maximum experienced by the sediment, and it appears that fluid sources such as petroleum generation continue after basins have become quiescent or begun eroding (Bredehoeft, Wesley, and Fouch, 1994). Microbially mediated porosity loss, which is probably restricted to temperatures less than 100°C (see table 1), may be reinitiated in rocks as they are uplifted and cooled. Finally, tectonic deformation probably also plays an important role in some instances. The mix of sometimes competing processes which can be present helps explain the complex and sometimes perplexing pattern of both high and low abnormal pressures observed in these environments.

Sedimentary basins in the Rocky Mountain region of North America, venues of both abnormally high and abnormally low pressures, are good examples of some of the geologic forcings described above. Spencer (1987) has postulated that high pressures in several basins, including the Piceance, Uinta, Green River, Wind River, Powder River, Big Horn, and Williston, are due to ongoing oil and gas generation providing fluid sources. Spencer based his assessment on the distribution of organic sources and the thermal history of the sediments. He also argued that although density effects may have caused high pressures locally, that "only active generation of hydrocarbons adequately explains basinwide, deep overpressure."

Numerical simulations done by Bredehoeft, Wesley, and Fouch (1994) of the Uinta Basin suggests that the conversion of solid kerogen to petroleum indeed generated the high abnormal pressures observed. The loss of kerogen creates porosity but tends to increase pressure because petroleum is less dense than kerogen. This is another instance where J/ρ exceeds $(\partial n/\partial t)^*$ in (17). Bredehoeft, Wesley, and Fouch (1994) noted that the reactions driving this process are strongly controlled by temperature. At relatively low temperatures Γ is too small to perturb the pressure. At relatively high temperatures, the kerogen is consumed too rapidly to produce long-lived forcing. This places fairly narrow constraints on the thermal history of the basin.

Abnormally low fluid pressures are quite conspicuous in the western Canada sedimentary basin (Hitchon, 1969b; Corbet and Bethke, 1992) and have also been observed in the Pierre Shale on the southern flank of the Williston Basin (Neuzil, 1993). Although Hitchon (1969b) attributed the low pressures in the western Canada basin to osmosis, Corbet and Bethke (1992) have used numerical simulations to show that they can be explained as a response to erosional unburdening. Erosion reverses the mechanical and thermal loading that occurs during deposition, causing decompaction and cooling of the underlying rock. These processes are described by (16) when $\partial \sigma_t/\partial t$ and $\partial T/\partial t$ are negative; in the shales of Western Interior North America, the stress changes dominate (Corbet and Bethke, 1992; Neuzil, 1993). Heuristically, fluid pressure decreased because expansion of the porous matrix and the resulting increase in porosity occurred more rapidly than pore fluid could flow in.

The abnormally low pressure present in the Pierre Shale is an unusual example of hydrodynamic disequilibrium occuring entirely within a relatively homogeneous shale (fig. 8). In addition, the shale properties and erosional forcing were unusually well constrained. Simulations of the system implied, with little ambiguity, that the abnormally low pressures are due to erosional unburdening and decompaction. Note that the Pierre Shale clearly displays the type of hydraulic head pattern expected for a distributed sink in a simple, homogeneous stratum (compare fig. 8 with fig. 5).

Orogenic zones and active plate boundaries.—Occasionally, abnormal pressures appear to be attributable wholly or substantially to tectonic deformation. Typically, these instances are associated with tectonically active convergent plate boundaries and related orogenic zones. Hubbert and Rubey (1959) mentioned several tectonically active regions known to have abnormally high pressures, including the foothills of the Andes in Argentina, the Himalayan foothills in Pakistan, and oil fields in Iran, Trinidad, and Burma.

Tectonic forces cause volumetric strain in rock, and some fraction of the strain is accommodated by a change in the porosity with an accompanying tendency to change fluid pressure. Strain rates are usually better known than stress history. As a result, the forcing is most usefully expressed in terms of the strain rate and can be written as

$$\Gamma = -\zeta_m \frac{\partial \sigma_t}{\partial t} = -\xi\dot{\epsilon}, \tag{18}$$

where $\xi = 1 - (K/K_s)$, the volumetric strain rate is denoted by $\dot{\epsilon}$, and compressional strain is defined to be positive.

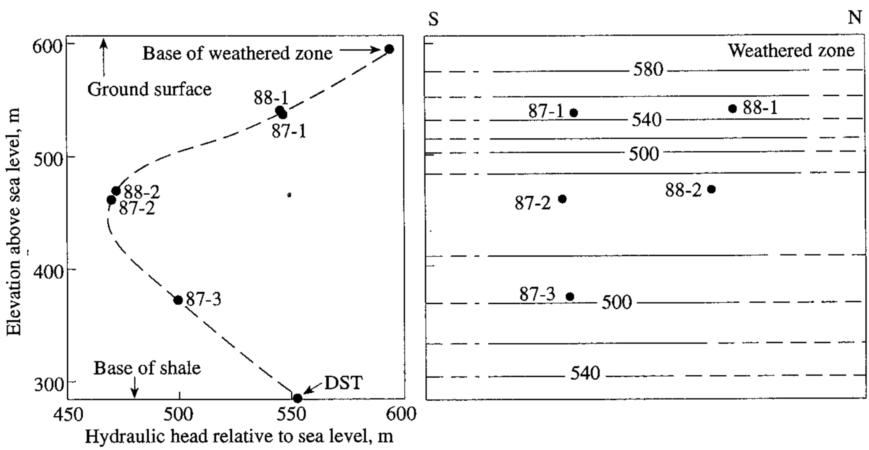

Fig. 8. Disequilibrium-type abnormal pressure in the Pierre Shale in central South Dakota. Left: hydraulic head with depth in the shale from all measurements; right: hydraulic head in a north-south cross section. All values are in meters above sealevel (reproduced from Neuzil, 1993, fig. 4).

Strain rates have been deduced in a number of ways. At convergent plate boundaries, the rates of relative plate movement and boundary geometry permit strain rates to be estimated with some confidence. In other instances, seismicity or accumulated strain sometimes permit estimates of strain rates. Some uncertainty results when it is necessary to estimate the volumetric strain rate $\dot{\epsilon}$ from an observed linear strain rate. As table 1 reveals, tectonic strain rates vary quite widely. Stable plate interiors and passive margins may experience a relatively minor tectonic forcing of 10^{-23} to 10^{-18} s^{-1}, which is probably insufficient to affect fluid pressures, except perhaps in unfractured crystalline rocks. Active portions of the crust like orogenic zones and active plate boundaries can have much more intense forcing (Ge and Garven, 1992; Garven and others, 1993). I will describe two instances of abnormal pressuring attributed to tectonic forcing, the California Coast Ranges and the Barbados accretionary complex, which serve to give some idea of the range of environments where tectonic forcing could be important.

Berry (1973) reported what appears to be an elongate region of abnormally high fluid pressures in the California Coast Ranges, paralleling the transform fault plate boundary in that region. The high pressures, which approach lithostatic values, are best developed in the low-permeability fine-grained sediments of the Franciscan sequence. Berry (1973) crudely delineated the high pressures using drilling data, and Unruh and others (1992) noted high elevation saline springs associated with thrust faults that are further indications of their presence. Davisson, Presser, and Criss (1994) also studied the springs and described geochemical evidence for high fluid pressures at depths of at least several kilometers. The Franciscan sediments are bounded by granitic blocks, which Berry (1973) speculated are compressing them from the northeast and southwest, normal to the faults. He had no measurements of the strain rates or permeability for this system, so his interpretation is speculative. However, it does not seem unreasonable. If one assumes a tectonic forcing of 10^{-15} s^{-1} on the basis of table 1 and a thickness of the Franciscan sediments of 10 to 15 km as reported by both Berry (1973) and Unruh and others (1992), inequality (15) suggests that abnormally high pressures will be generated if the Franciscan permeability is 10^{-18} m^2 or lower ($\kappa < 10^{-11}$ ms^{-1}). This is a quite reasonable value for fine-grained sediments.

Screaton, Wuthrich, and Dreiss (1990) analyzed sediment deformation and fluid flow in the Barbados accretionary complex. They cite high fluid pressures during drilling, fluidized sediments, and signs of fluid expulsion as evidence of near-lithostatic pressures in the complex. Geochemical and geothermal evidence for abnormally high pressures was discussed by Vrolijk, Fisher, and Gieskes (1991). Convergent margins like the Barbados complex are loci of intense deformation, where thick prisms of sediments are scraped from the subducting oceanic plate, as shown in figure 9. Screaton, Wuthrich, and Dreiss (1990) simulated the deformation of sediments and resulting movement of fluids in the

Barbados complex using the rate of plate convergence and the system geometry to constrain the rate of porosity loss. One result of their analysis, a map of Γ, is reproduced in the bottom part of figure 9. This map clearly illustrates an aspect of geologic forcing that is probably significant in many environments: its spatial variation. For the range of Γ shown in figure 9, approx 3×10^{-16} to 3×10^{-14} s^{-1}, Screaton, Wuthrich and Dreiss (1990) found that appropriately high fluid pressures were generated when permeabilities are between 10^{-17} and 10^{-19} m^2 (κ between 10^{-10} and 10^{-12} ms^{-1}) (also see fig. 6).

Deep crystalline rock.—The disequilibrium-type abnormal pressures discussed so far have been restricted to sedimentary terrains. There is scant evident for significant hydrodynamic disequilibrium in crystalline rocks at depths of a few kilometers or less. Presumably these rocks are too pervasively fractured, and thus too permeable, to permit natural disequilibrium to be generated. However, there is evidence that at depths around 10 km in crystalline rock terrains, even in stable continental shields, abnormally high pressures exist. At these depths the high temperatures and stresses may prevent or heal fractures and probably drive diagenetic porosity reduction in the form described by (17). Walder and

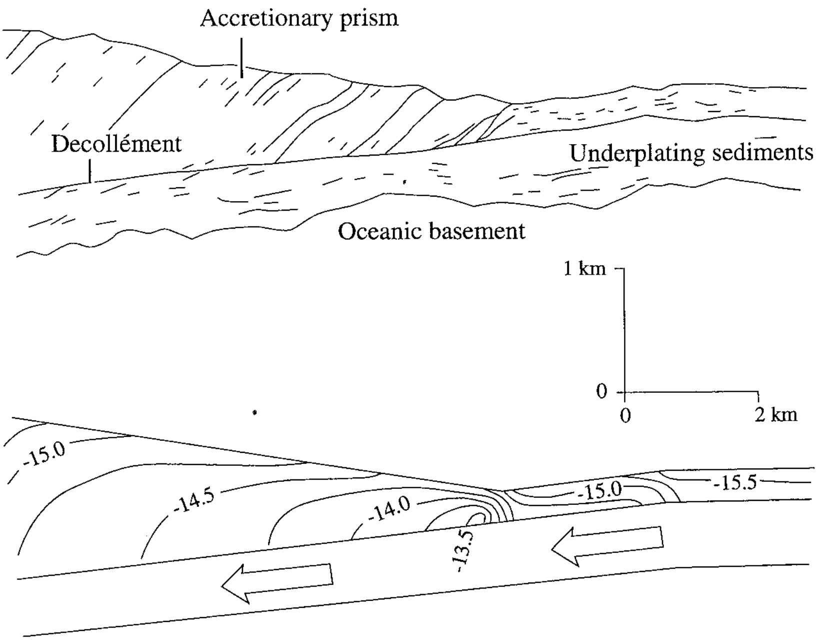

Fig. 9. West to east cross sections through the Barbados accretionary complex showing the structure interpreted from seismic and drilling data (top) and values of log Γ in s^{-1} (bottom). The top cross section was adapted from that of Vrolijk, Fisher, and Gieskes (1991) and the bottom presents simulation results obtained by Screaton, Wuthrich, and Dreiss (1990).

Nur (1984) speculated that pressure solution is the particular mechanism reducing the porosity in these environments. Tectonic forcing, as described by (18), sometimes may also play a role.

The most direct evident for abnormal pressures in deep crystalline rock comes from the superdeep borehole on the Kola Peninsula in Russia. The borehole is reported to have encountered abnormally high pressure fluids, presumably in fractures, at approx 9 km depth (Borevsky, Vartanyan, and Kulikov, 1984). Additional, indirect evidence comes from seismic studies of the crust. Experiments by Nur and Simmons (1969) and Todd and Simmons (1972) have shown that in saturated, low-porosity rocks, compressional wave velocity drops noticeably as the fluid pressure approaches the total stress on the specimen. In view of these results, Berry and Mair (1977) hypothesized that near-lithostatic abnormal fluid pressures would cause zones of low seismic velocity in the crust. Conversely, low-velocity zones may delineate regions of abnormally high fluid pressure.

Low-velocity zones between 7 and 12 km depth are prominent features in seismic profiles obtained in regions as diverse as northern Europe, South Africa, eastern and western United States, Australia, Japan, the Baltic Shield, and the Canadian Shield (Mueller and Landisman, 1966; Berry and Mair, 1977). Indeed, evidence for such a feature is so widespread that Mueller and Landisman speculated that it may be nearly ubiquitous in the continental crust.

The Canadian Shield may offer the most clearly mapped example of a low-velocity zone. A detailed seismic study of the crust carried out near Yellowknife, Northwest Territories was analyzed by Clee, Barr, and Berry (1974) and Berry and Mair (1977). A cross section of the crust showing a prominent low velocity zone between 8 and 10 km depth was deduced from their analysis and is shown in figure 10. Notice that the low-velocity (and perhaps abnormally pressured) zone is present in the granitic rock but does not extend into the adjacent greenstones.

Neither the permeability nor the strength of the forcing in any low-velocity zones had been measured. Walder and Nur (1984) used the permeability of unfractured crystalline rock, which they took to be 5×10^{-20} m^2 (κ of 5×10^{-13} ms^{-1}), to calculate that $(\partial n/\partial t)^*$ must be between 10^{-16} and 10^{-15} s^{-1} to generate the supposed abnormal pressures. At permeabilities as much as 10^4 times smaller, which were measured by Trimmer and others (1980) in granite and gabbro, much smaller forcings (between 10^{-20} and 10^{-16} s^{-1}) would suffice to generate abnormal pressures (see fig. 6).

EXTRACTING INFORMATION FROM ABNORMAL PRESSURE REGIMES

The Inverse Problem: Abnormal Pressures and Permeability

In rare instances it is possible to identify low-permeability regions using very indirect techniques, such as rock-water ratios during metamorphism (for example, Ferry and Dipple, 1991). For the most part, however, it is extremely difficult to characterize or even to detect low

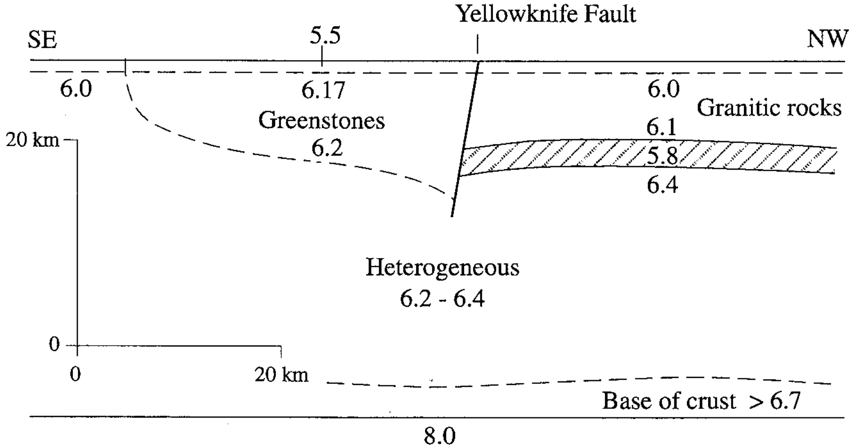

Fig. 10. Southeast to northwest cross section showing the seismic velocity structure of the Canadian Shield in the vicinity of Yellowknife, Northwest Territories. Velocities are in km s^{-1}. A prominent low-velocity zone (5.8 km s^{-1}) is present in the granitic rocks (adapted from Clee, Barr and Berry 1974, fig. 17).

permeability at large scales. Mapping a lithology with intrinsically low permeability tells little about large-scale behavior because of the influence of transmissive fractures and stratigraphic or structural heterogeneities. It is impractical, moreover, to hydraulically test low-permeability media except at small scales (Neuzil, 1986). Therefore the linkage between abnormal pressures of all types and regions of low permeability, as defined by the hydrodynamic model, is potentially very useful. This section explores abnormal pressures in relation to the inverse problem of delineating regions of low permeability and evaluating their hydraulic properties.

Low-permeability barriers in equilibrated flow systems.—Abnormal pressures in equilibrated flow regimes have proven to be quite useful for evaluating flow across low-permeability strata, which allows estimation of the vertical (or cross-stratification) permeability over quite large regions. This is possible because the low-permeability strata act like the walls of a leaky conduit; leakage through these units is an important control of the hydrodynamics of the system. Analysis of a system sometimes constrains the rate of leakage. In flow systems that are reasonably well understood, the quality of information about the low-permeability strata and level of detail that can be obtained are surprisingly good. This is nicely shown by two studies of contiguous abnormal pressure systems in the Western Interior of North America.

Bredehoeft, Neuzil, and Milly (1983) and Belitz and Bredehoeft (1988) simulated flow in the sedimentary sections of the south flank of the Williston Basin and the adjoining Denver Basin respectively. In this region, a sequence of Cretaceous shales overlies the Dakota Sandstone, which has abnormally low pressures in the Denver Basin (as portrayed earlier in fig. 2) and abnormally high pressures in South Dakota. In both regions, analyzing the abnormal pressures as equilibrium hydrodynamic phenomena in a topographically-driven flow system allowed the permeability of the Cretaceous shales to be estimated.

Figure 11A synthesizes the results of the two studies in a single north-south cross section. The regional vertical permeability of the shale in the Denver Basin (right side of fig. 11) is quite low, less than 3×10^{-20} m^2. The regional vertical permeability of the shale sequence in South Dakota is on the order of 10^{-18} m^2, or at least a hundred times greater. This could indicate large-scale areal heterogeneity in the hydraulic properties of the Cretaceous shale sequence, as suggested by figure 11A. However, another interpretation of the results, illustrated in figure 11B,

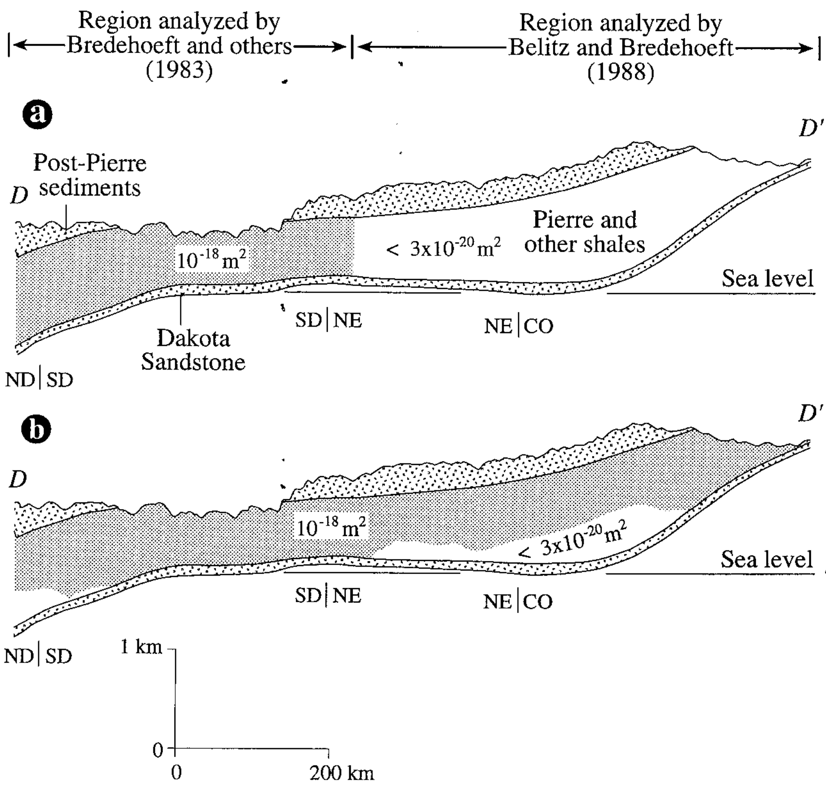

Fig. 11. North to south cross section of the Cretaceous shales and underlying Dakota Sandstone showing regional permeability estimates. (A) The permeability estimates as obtained from the regional flow studies. (B) A conceptual model that explains the areal permeability differences by making permeability a function of depth. The cross section was constructed using information from the Petroleum Information Corporation and other sources. The location of the cross section is shown in figure 14.

is that the entire shale sequence is vertically zoned with respect to permeability, and the deepest shale is also the least permeable. The latter interpretation is supported by the finding of Bredehoeft, Neuzil, and Milly (1983) that individual shale units in South Dakota have decreasing regional vertical permeability with depth.

Disequilibrium and hydraulic isolation.—The criterion for generating abnormal pressures as hydrodynamic disequilibria, presented earlier as inequality (15), is $\kappa/l < |\Gamma|$. This derives from analyses of idealized systems, where a single valued, scalar κ characterizes the entire domain. Homogeneity and isotropy represent a considerable simplification of most geologic environments. Indeed, most data on abnormal pressures have come from fluid pressure measurements in rather permeable geologic units. Obviously, the critical property of disequilibrium domains is isolation from their surroundings by low-permeability units or regions and not necessarily the presence of a uniformly low-permeability volume of rock. Fortunately, the criterion expressed by inequality (15) also describes more complex domains where κ characterizes only the low-permeability components. This is because the forcing generally acts over the entire domain, including any permeable regions, while the pressure dissipation is controlled by the least permeable unit that the flow must cross to dissipate the disequilibrium.

Surveying abnormal pressures interpreted as disequilibria, it can be surmized that a highly varied set of permeability patterns permits the required degree of hydraulic isolation. As one might expect, the patterns reflect sedimentary architecture, geologic structure, deformation, diagenesis, and so forth. Generalization is difficult, but the patterns of permeability in which disequilibrium occurs can be broadly viewed as constituting a continuum marked by various ratios of high- to low-permeability rock. This continuum is depicted schematically for both sedimentary and crystalline terrains, in figure 12.

Permeability patterns seem to have fractal properties, so the patterns shown in figure 12 represent various scales. Sometimes, different parts of the continuum shown in figure 12 can characterize the same environment at different scales. For example, the low-permeability subregions shown in the right-hand side of figure 12 may, at smaller scales, be properly placed in the center or left-hand side of figure 12. Such relationships have in fact been observed; Hunt (1990) describes low-permeability zones containing minor reservoirs which lie between thick, extensive reservoirs. A "low-permeability region" marked by the presence of disequilibrium abnormal pressure thus may be complexly heterogeneous on more than one scale. Despite their complexity, however, such domains clearly can have no permeable connections to normally pressured surroundings.

Relatively few disequilibrium pressure regimes have been reported in environments where permeable units are rare or absent (fig. 12, left). Notable exceptions are the underpressured regime in the Pierre Shale described earlier and shown in figure 8, as well as an abnormally low

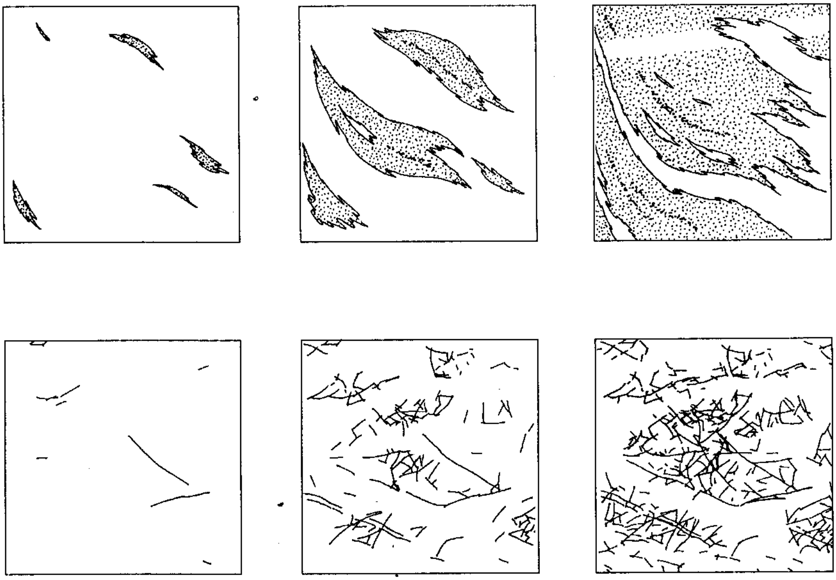

Fig. 12. Schematic drawings depicting the continuum in permeability patterns that permit generation and maintainance of hydrodynamic disequilibrium. White regions are low-permeability rock, and the upper drawings represent hypothetical sedimentary sequences, while the lower drawings represent hypothetical fracture patterns in crystalline rock. Simple low-permeability domains with minor permeable components at the left grade into more complex patterns, were permeable rock is volumetrically dominant but is isolated by low permeability components. The fracture patterns were adapted from a lineament map by Gustafsson (1994).

pressure regime in the Valinginian Marl in Switzerland (Vinard and others, 1993), and abnormally high pressures in thick evaporites in New Mexico (Peterson, Lagus, and Lie, 1987). Although the paucity of examples seems to imply that homogeneous low-permeability environments are not common, they are probably underrepresented in the gathering of data. A distinguishing feature of these environments is the fact that fluid pressures must be measured in low-permeability lithologies, a difficult and costly procedure that is done very infrequently. Bradley (1975) not long ago observed that "there has never been a measurement of the [fluid] pressure in a shale," and there are still few exceptions to this statement. Indirect measures imply that relatively homogeneous low-permeability domains with abnormal pressures are not particularly rare. Undercompacted shales, revealed either by their tendency to flow into the borehole (Pritchett, 1980) or by unexpectedly high porosity at depth (Magara, 1968; Gretener and Feng, 1985) frequently are an indication of abnormally high fluid pressure. Also, the abnormally high pressures at several kilometers depth inferred by Berry and Mair (1977) from seismic data may occur in relatively homogeneous, unfractured crystalline rock.

The great majority of known disequilibrium-type abnormal pressures appear to be in environments with significant permeable components. A commonly encountered sedimentary architecture that gives rise to this condition is sandstone or carbonate strata enclosed in argillaceous sediments. According to Corbet and Bethke (1992) the abnormally underpressured Cretaceous sediments of the western Canada sedimentary basin are an example of this. Many geopressures in actively subsiding basins apparently are in similar settings; Harrison and Summa (1991) note that Gulf Coast geopressures are developed where permeable sands comprises something more than 10 percent of the sediment. Isolation of permeable units also occurs where faulting and soft-sediment deformation disrupt their continuity. The Barbados accretionary complex described by Screaton, Wuthrich and Dreiss (1990), where the sedimentary structure has been greatly disturbed by lateral compression, deformation, and thrusting, appears to be an example of this. It should also be noted that similar permeability patterns are possible in crystalline rocks if isolated fracture clusters are present (fig. 12, bottom). The abnormally high pressures in the Kola superdeep borehole (Borevsky, Vartanyan, and Kulikov, 1984) apparently occurred in one or more clusters of fractures, because significant quantities of water had to flow into the borehole to be detected.

At increasingly large volume fractions of permeable rock, the likelihood of permeable connections through a region increases. However, disequilibrium-type abnormal pressures are known to exist where permeable rock predominates, indicating that hydraulic isolation occurs under these conditions. Often, these systems are distinguished by their incorporation of permeable abnormally pressured subunits large enough to display internal hydrostatic pressure gradients. Pressure and hydraulic head profiles in such a domain are shown in figure 13. The head profile in figure 13 may be contrasted with that in a homogeneous domain (figs. 5 and 8). The abnormal pressure indicates overall enclosures within low-permeability units while the hydrostatic gradient indicates internal hydraulic communication in comparatively permeable media. Pressure patterns suggestive of these circumstances have been reported in sedimentary basins around the world. Rehm (1972) shows many cases where drilling mud weights suggest elevated but essentially constant heads over hundreds to thousands of meters depth. These pressure patterns are often attributed to the seal phenomenon already described. In particular, pressure seals in complex three-dimensional patterns have been invoked to explain regimes with distinct abnormal pressures that appear to adjoin each other laterally as well as vertically (Rehm, 1972; Hunt, 1990; Powley, 1990). The latter have been termed "pressure compartments."

Crustal permeability patterns.—Our knowledge of the occurrence of abnormal pressures is incomplete. In particular, drilling and testing generally have provided few pressure data in low-permeability units, at depths exceeding 7 or 8 km, or outside of suspected or known hydrocarbon provinces. Nevertheless, the extant data on abnormal pressures yield insight into the distribution of permeability in the crust. I anticipate that this insight will deepen as additional data are obtained and systematic analyses based on hydrodynamics are undertaken.

Within 7 to 10 km of the surface the occurrence of low-permeability regions appears to be related to the type of geologic terrain. There are few, if any, abnormal pressures in crystalline terrains, probably because these media are pervasively fractured and relatively permeable at moderate stresses and temperatures. In sedimentary terrains, on the other hand, low-permeability domains indicated by abnormal pressures are reasonably common in the upper several kilometers of the crust. They seem to occur most frequently in relatively young accumulations of sediment, perhaps because these are least likely to maintain transmissive fractures.

At depths of approx 7 km and greater, permeable rock may be uncommon. According to Powley (1990), most thick sedimentary accumulations host abnormal pressures at depths of several kilometers, and as I have already noted, seismic evidence suggests that there may be pervasive high pressures (and by implication low permeabilities) between 7 and 12 km depth. There is some difficulty reconciling this interpretation with evidence for deep circulation of water (for example, that described by Taylor, 1990). Nur and Walder (1990) recognized this difficulty and proposed that deep, low-permeability regimes are cyclically fractured and resealed. According to them, deep circulation of groundwaters "represent only the periods or episodes of fast flow and not the crust in general."

In places, low-permeability regions in sediments of the shallow crust could be continuous with deeper, regional low permeability. This possibility has already been mentioned with respect to the U.S. Gulf Coast. Other abnormal pressures clearly have normal pressures beneath them, such as those in the Green River Basin shown in figure 13, indicating that they are disconnected from low permeability at greater depths by intervening permeable rocks. A generalized permeability map of the continental crust would, therefore, include a very extensive and possibly continuous zone of low permeability at a depth of 7 to 12 km which occasionally protrudes into shallower regions of the crust, plus discrete low-permeability regions "floating" in permeable upper crustal rock.

Western Interior North America provides a specific example of how abnormal pressure regimes might be used to map permeability regionally. Figure 14 shows the areal distribution of low permeability ($<10^{-18}$ m^2) in this region inferred from both equilibrium and disequilibrium type abnormal pressure regimes that have been discussed in this paper. The map reveals a permeability heterogeneity on the scale of hundreds to thousands of kilometers. The low-permeability regions shown are in the upper 2 to 5 km of sedimentary cover and are not continuous with any deeper low-permeability zones that may be present. The most extensive low-permeability regions (fig. 14, 1 and 2), are associated with Cretaceous shales in the foreland basins of the Rocky Mountains. It is sometimes'

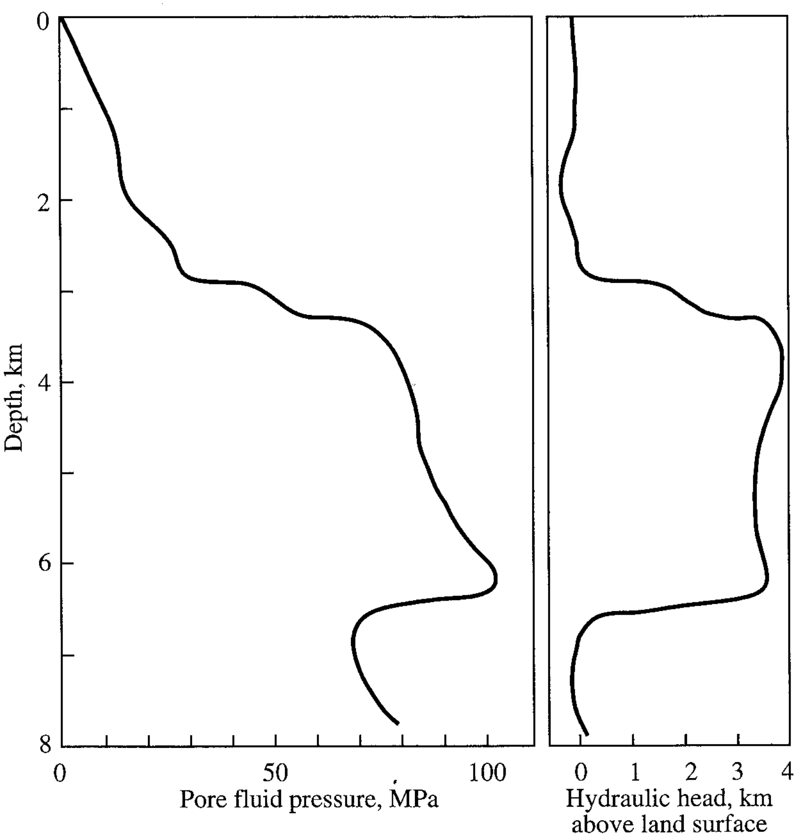

Fig. 13. Pore fluid pressure and hydraulic head with depth in the Pacific Creek area, Green River Basin, Wyoming. The abnormally pressured section suggests the presence of a 3-km-thick permeable zone, with internal hydrostatic pressure gradient, isolated by relatively thin low-permeability zones above and below. Pressures were interpreted by Spencer (1987) based on mud-weights, drill-stem tests, and other data.

possible to deduce the vertical permeability pattern as well as the areal; figure 11 has already shown this along transect D–D′ of figure 14.

The Detection Problem: Abnormal Pressures and Geologic Processes

According to the hydrodynamic model, disequilibrium-type abnormal pressures integrate the effects of geologic processes that tend to perturb the fluid pressure. By extension, disequilibrium regimes contain information about these geologic processes and their history. In some instances abnormal pressures point to the presence of geologic forcing which could otherwise be overlooked or constrain the value of Γ temporally and spatially. An example is abnormally high fluid pressures in the Uinta Basin that result from petroleum generation and imply a rather

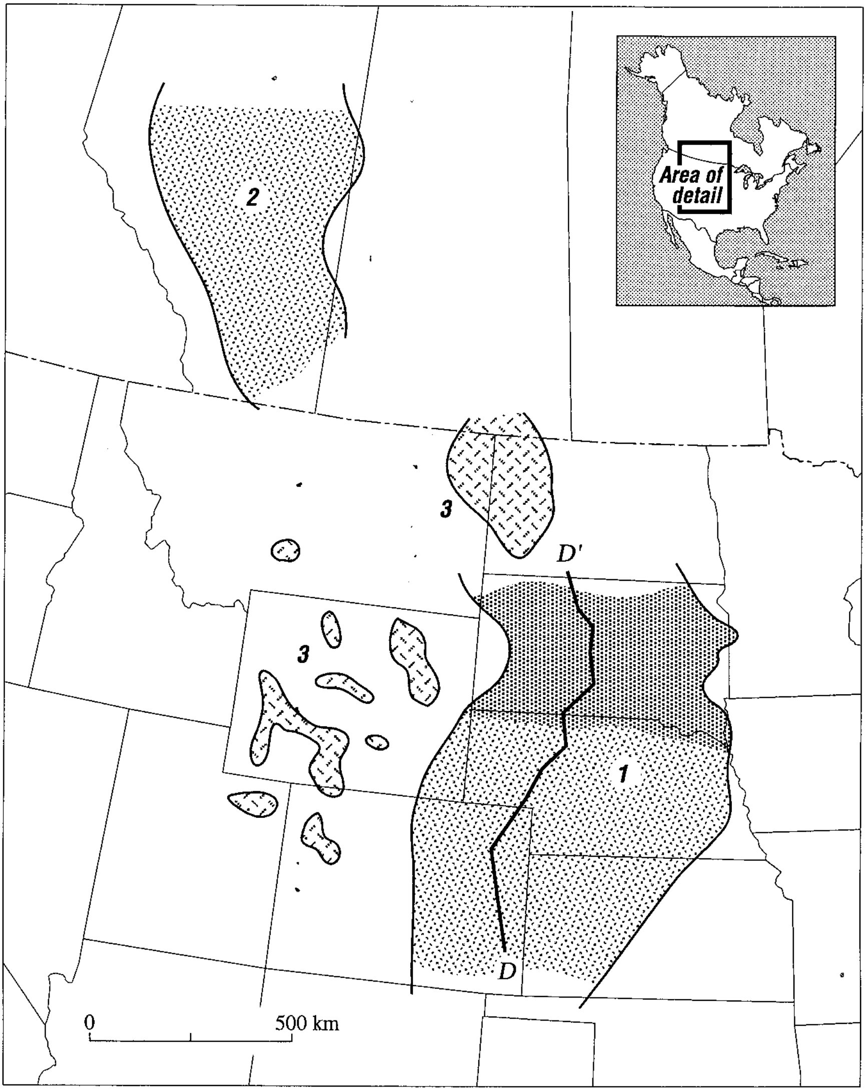

Fig. 14. Map of the western interior of North America showing low permeability ($< 10^{-18}$ m^2) regions inferred from abnormal pressures: (1) (northern part) shale sequence with a regional vertical permeability of 10^{-18} m^2 (Bredehoeft, Neuzil, and Milly, 1983); (southern part) shale sequence with a regional vertical permeability smaller than 3×10^{-20} m^2 (Belitz and Bredehoeft, 1988); (2) one or more shales with regional permeability of approx 10^{-20} m^2; (3) domains hydraulically isolated by permeabilities of 10^{-18} m^2 or smaller (assuming $\Gamma < 10^{-14}$ s^{-1}; these regions may actually be clusters of smaller low-permeability domains) (Spencer, 1987; Bredehoeft, Wesley, and Fouch, 1994). D–D′ denotes location of section depicted in figure 11.

specific thermal history for the sediments there (Bredehoeft, Wesley, and Fouch, 1994). Another example is the inferred widespread high fluid pressure at 7 to 12 km depth; active porosity reduction probably would not be suspected in this environment without the indications of abnormal pressures.

Unfortunately, the nature of the detection problem dictates strong limitations to the information one can extract about past geologic activity. Hydrodynamic disequilibrium is dominated by the most recent forcing as the fingerprint of geologic processes grows increasingly faint with time. This exacerbates a nonuniqueness that is introduced by uncertainty in system properties and geometry. The limitations are evident in my study of abnormally low fluid pressures in the Pierre Shale (Neuzil, 1993). In that study, the shale properties (permeability, porosity, and compressibility), geometry, and pressure regime were well established by drilling, sampling, and testing. Analysis of the flow disequilibrium clearly indicated erosion as the forcing process and broadly constrained the erosion rate over the past 10^5 yrs. However, it was not possible to determine the total amount of erosion or to distinguish between several different erosion histories for the past 2 my (Neuzil, 1993).

DISCUSSION

Unlike the hydrodynamic model, the static model suggests that abnormal pressures are not dissipated by flow, obviating the need for ongoing pressure perturbation. The static model itself encompasses different conceptual approaches. For example, some researchers have suggested that abnormal pressures are generated by long-term maintainance of fluid pressure itself, rather than simply containment of fluid mass. When a region becomes hydraulically isolated (as by the formation of seals) pressures that were originally hydrostatic thereby become abnormally high or low as the geologic framework evolves. Bradley (1975) depicts such an origin for abnormally high pressure: as the land surface is eroded, subsurface pressures remain at the hydrostatic value for the old higher land surface. This phenomenon would aptly be described as fossil pressure or paleopressure. More frequently, however, the static model sees fluid pressures as changeable; geologic processes generate abnormal pressures and may continue to alter them over time, but fluid mass is contained. Because of the containment, abnormal pressures are preserved during periods of geologic quiescence. An example of the latter approach is Barker's (1972) aquathermal pressuring concept, wherein thermal expansion of pore fluid during subsidence is seen as generating high pressures. Both concepts, (1) fossil pressure and (2) long-term fluid containment, merit additional comment.

In my view, fossil pressures raise serious conceptual problems. It is difficult to imagine how to effect significant changes to the geologic framework without incurring significant pressure perturbations. During erosion or deposition, for example, mechanical and thermomechanical deformation change porosity and fluid density. Absolute pressures can be maintained in rocks that are very stiff or poorly deformable. However, this would require a very fortuitous set of circumstances (Neuzil, 1985). The preservation of fluid pressure, if it occurs at all, must be a rare circumstance.

The concept of fluid containment over geologic time raises different issues, which are both difficult and interesting. It can be approached in relative rather then absolute terms by posing the following question: how small must the permeability be to preserve abnormal pressures over significant spans of geologic time? I have already presented the analysis that allows one to approach this question. The dissipation of abnormal pressures by flow can be characterized using dimensionless time t_D. Disequilibrium (the abnormal pressure) is essentially "preserved" for $t_D < 0.1$. Using the definition of t_D, the required permeability (as hydraulic conductivity) can therefore be expressed as $\kappa \leq 0.1\ (S_s' l^2)/t$. Taking S_s' to be a representative $10^{-6}\ m^{-1}$, l to be 10^3 m, and requiring pressure to be maintained for 50 my ($t = 1.5 \times 10^{15}$ s) yields $\kappa < 6 \times 10^{-17}\ ms^{-1}$ or a permeability of less than $6 \times 10^{-24}\ m^2$.

Previous discussion of permeability suggests that this value is below the range indicated by the best recent measurements for argillaceous media, crystalline rocks, and most evaporites. Only the permeability of pure halite may meet this criterion. The concept of fluid containment postulated by the static model therefore does not seem to be supported by permeability data. A similar argument was made by Tóth and others (1991) in their discussion of the static model.

However, low permeability flow is a more complex issue than it at first appears. There is uncertainty about low-permeability flow behavior, particularly in argillaceous media. Various investigators have described threshold gradients and other non-Darcian behavior (see, for example, Mitchell and Younger, 1967; Elnagger, Karadi, and Krizek, 1974). These phenomena, reported in porous media saturated with water, are distinct from the well-established effects of capillarity in media containing more than one fluid phase. In a medium with a threshold gradient, flow does not occur unless the hydraulic head gradient exceeds a certain value; at lower gradients the medium appears to be impermeable. Typically, reported threshold gradients range between 1 and 100. If present, they could drastically affect flow in the subsurface, because hydraulic gradients in nature are usually less than 1. Byerlee (1990), for example, has shown that threshold gradients could maintain high fluid pressures in fault zones. However, the evidence for non-Darcian flow is controversial because definitive experiments have so far proven impractical. Little consideration has been given to this problem by currently active researchers, and in my opinion it remains unresolved (Neuzil, 1986). A role for threshold gradients or similar non-Darcian phenomena in abnormal pressuring therefore cannot be ruled out. All one can say is that with the hydrodynamic model it is not necessary to appeal to this additional complexity to explain abnormal pressures.

It is not at all clear that it will ever be possible to test definitively conceptual models for abnormal pressure. This is because (1) access to the subsurface is difficult and costly, commonly resulting in few data being available to characterize a system, (2) subsurface systems tend to be geologically and hydraulically complex, and (3) relevant dynamic processes cannot be observed on appropriate spatial and temporal scales. Adequate characterization of subsurface environments is a particular problem. An understanding of the geologic framework must be founded upon relatively sparse boreholes and indirect geophysical characterization. Subsurface pressure patterns are similarly uncertain. Many reported abnormal pressures are not based on pressure measurements at all but are deduced from geophysical logging or mud weights (Gretener and Feng, 1985). Most actual pressure data are obtained as rapidly as possible (for reasons of cost) and are thus of variable reliability, particularly in low-permeability formations. Moreover, pressure data are often obtained after human disturbance of a system, and it is difficult to know whether abnormal pressures reflect natural conditions or the injection or withdrawal of fluids.

Even where abnormal pressure regimes are relatively well defined, experience has shown that it can be difficult to establish the nature of the flow. The Denver Basin is an instructive case in point. A decade ago, Ottman (1984) concluded that the strikingly low hydraulic heads in the Cretaceous sandstones there (shown earlier in fig. 2) represented hydrodynamic disequilibrium caused by erosional unloading. The later study by Belitz and Bredehoeft (1988) showed that the low pressures are readily explained as occuring in an equilibrated flow regime. The different interpretations are critical not only for understanding the origin of the low pressures; they imply quite different regional permeability and flow patterns. Disequilibrium implies hydraulic isolation of the Cretaceous sandstones. Equilibrated, topographically-driven flow implies no such isolation. Indeed, it implies just the opposite; the Cretaceous sandstones of the Denver Basin may be abnormally pressured *because* they connect the basin interior with distant, low-elevation discharge points. This is particularly relevant to the perception that abnormal pressures must be indicative of "restricted" or "closed" systems (Gretener and Feng, 1985; Bradley, 1975; Powley, 1990; Hunt, 1990).

CONCLUSIONS

The hydrodynamic model that I have outlined in this paper provides a general framework for understanding abnormal pressures. It stems from a view of the Earth's crust as an ephemeral, continuously evolving structure in which flow regimes must also evolve. Equilibrated regimes have remained current, and disequilibrium regimes have lagged the changes. In the former, abnormal pressures would persist indefinitely in the absence of further changes to the geologic framework. In the latter, they must be maintained by active, ongoing geologic forcing involving porosity or temperature changes, fluid sources, or some combination of the three. Forcing sufficient to maintain abnormal pressures in low-permeability environments apparently arises in many different geologic settings, the result of a variety of natural processes. This helps explain why various abnormal pressure environments often appear to have little in common, an attribute on which Gretener and Feng (1985) have remarked.

The hydrodynamic model may enable one to extract fairly specific information about crustal hydraulic properties and processes. This is possible because abnormal pressure regimes are, in effect, large-scale, long-term analogues to hydraulic and mechanical tests that one might conduct in a borehole or in the laboratory. Because these natural "experiments" occur on long time scales, they offer information that would be impossible to obtain through human intervention. In particular, they can reveal the presence, nature, and extent of large low-permeability regions, which is a highly desirable capability. Such regions constrain regional groundwater flow, sequester sizeable quantities of water and chemical mass for significant periods of time, and are potentially advantageous as sites for hazardous-waste disposal.

Uncertainty will undoubtedly continue to characterize analyses of specific abnormal pressure regimes, limiting the amount of information that can be gained from them. However, hydrodynamics provides the tools for understanding abnormal pressures as a class of phenomena. It seems likely that systematic examination of abnormal pressures and analysis of them using the hydrodynamic model will yield significant and perhaps crucial new knowledge pertaining to problems of fluid movement in the crust. These problems are of both scientific and practical interest. Subsurface fluids play important roles in the generation of economic mineral deposits and the structural development of the crust. Groundwater and hydrocarbons are vital to society. Intelligent exploitation of the subsurface will be hindered without an understanding of the development and behavior of abnormal pressures.

ACKNOWLEDGMENTS

This paper took its present form in discussions with John Bredehoeft; I am grateful for these insightful exchanges. I am also indebted to Grant Garven, Craig Bethke, Tom Reilly, Terry Engelder, Peter Gretener, and an anonymous reviewer for their comments. Responsibility for the ideas expressed, as well as for any errors, remains mine.

REFERENCES

Anderson, J. G., 1986, Seismic strain rates in the central and eastern United States: Bulletin of the Seismological Society of America, v. 76, p. 273–290.

Angevine, C. L., and Turcotte, D. L., 1983, Porosity reduction by pressure solution: A theoretical model for quartz arenites: Geological Society of America Bulletin, v. 94, p. 1129–1134.

Barker, C., 1972, Aquathermal pressuring—role of temperature in development of abnormal-pressure zones: American Association of Petroleum Geologists Bulletin, v. 56, p. 2068–2071.

Beauheim, R. L., Saulnier, G. J., Jr., and Avis, J. D., 1991, Interpretation of brine-permeability tests of the Salado Formation at the waste isolation pilot plant: First interim report: Albuquerque, New Mexico, Sandia National Laboratory, Sandia Report SAND90-0083, 205 p.

Belitz, K., and Bredehoeft, J. D., 1988, Hydrodynamics of Denver Basin: Explanation of subnormal fluid pressures: American Association of Petroleum Geologists Bulletin, v. 72, p. 1334–1359.

Berry, F. A. F., ms, 1959, Hydrodynamics and geochemistry of the Jurassic and Cretaceous systems in the San Juan Basin, northwestern New Mexico and southwestern Colorado: Ph.D. thesis, Stanford University, 213 p.

———— 1973, High fluid potentials in California coast ranges and their tectonic significance: American Association of Petroleum Geologists Bulletin, v. 57, p. 1219–1249.

Berry, F. A. F., and Hanshaw, B. B., 1960, Geologic field evidence suggesting membrane properties of shales [abstract]: International Geological Congress, 21st, Norden, Germany, Report of Sessions, p. 209

Berry, M. J., and Mair, J. A., 1977, The nature of the Earth's crust in Canada, *in* Heacock, J. G., editor, The Earth's Crust, its Nature and Physical Properties: American Geophysical Union, Geophysical Monograph 20, p. 319–348.

Bethke, C. M., 1986, Inverse hydrologic analysis of the distribution and origin of Gulf Coast-type geopressured zones: Journal of Geophysical Research, v. B91, p. 6535–6545.

———— 1989, Modeling subsurface flow in sedimentary basins: Geologische Rundschau, v. 78, p. 129–154.

Biot, M. A., 1941, General theory of three-dimensional consolidation: Journal of Applied Physics, v. 12, p. 155–164.

Borevsky, L. V., Vartanyan, G. S., and Kulikov, T. B., 1984, Hydrogeological essay, *in* Kozlovsky, Ye. A., editor, The Superdeep Well of the Kola Peninsula: New York, Springer-Verlag, p. 271–287.

Brace, W. F., 1980, Permeability of crystalline and argillaceous rocks: International Journal of Rock Mechanics and Mining Science, v. 17, p. 241–245.

Bradley, J. S., 1975, Abnormal formation pressure: American Association of Petroleum Geologists Bulletin, v. 59, p. 957–973.

Bredehoeft, J. D., 1988, Will salt repositories be dry? EOS (Transactions of the American Geophysical Union), v. 69, p. 121–131.

Bredehoeft, J. D., and Hanshaw, B. B., 1968, On the maintenance of anomalous fluid pressures: I, Thick sedimentary sequences: Geological Society of America Bulletin, v. 79, p. 1097–1106.

Bredehoeft, J. D., Neuzil, C. E., and Milly, P. C. D., 1983, Regional flow in the Dakota Aquifer: A study of the role of confining layers: U. S. Geological Survey Water-Supply Paper 2237, 45. p.

Bredehoeft, J. D., and Norton, D. L. 1990, Mass and energy transport in a deforming Earth's crust, *in* Bredehoeft, J. D., and Norton, D. L., editors, The Role of Fluids in Crustal Processes: Washington, D. C., National Academy Press, p. 27–41.

Bredehoeft, J. D., Wesley, J. B., and Fouch, T. D., 1994, Simulation of the origin of fluid pressure, fracture generation, and the movement of fluids in the Uinta Basin, Utah: American Association of Petroleum Geologists Bulletin, v. 78, p. 1729–1747.

Byerlee, J., 1990, Friction, overpressure and fault normal compression: Geophysical Research Letters, v. 17, p. 2109–2112.

———— 1993, Model for episodic flow of high-pressure water in fault zones before earthquakes: Geology, v. 21, p. 303–306.

Capuano, R. M., 1993, Evidence of fluid flow in microfractures in geopressured shales: American Association of Petroleum Geologists Bulletin, v. 77, p. 1303–1314.

Carslaw, H. S., and J. C. Jaeger, 1959, Conduction of Heat in Solids: London, Oxford University Press, 510 p.

Clee, T. E., Barr, K. G., and Berry, M. J., 1974, Fine structure of the crust near Yellowknife: Canadian Journal of Earth Science, v. 11, p. 1534–1549.

Corbet, T. F., and Bethke, C. M., 1992, Disequilibrium fluid pressures and groundwater flow in the western Canada sedimentary basin: Journal of Geophysical Research, v. B97, p. 7203–7217.

Davisson, M. L., Presser, T. S., and Criss, R. E., 1994, Geochemistry of tectonically expelled fluids from the northern Coast Ranges, Rumsey Hills, California, USA: Geochimica et Cosmochimica Acta, v. 58, p. 1687–1699.

Dickinson, G., 1953, Geological aspects of abnormal reservoir pressures in Gulf Coast Louisiana: Bulletin of the American Association of Petroleum Geologists, v. 37, p. 410–432.

Domenico, P. A., and Palciauskas, V. V., 1979, Thermal expansion of fluids and fracture initiation in compacting sediments: Geological Society of America Bulletin II, v. 90, p. 953–979.

Elnagger, H. A., Karadi, G. M., and Krizek, R. J., 1974, Non-Darian flow in clay soils, *in* Stoll, H. W., editor, Flow, Its Measurement and Control in Science and Industry, vol. 1, Flow Characteristics: Pittsburgh, Instrument Society of America, p. 53–61.
Ferry, J. M., and Dipple, G. M., 1991, Fluid flow, mineral reactions, and metasomatism: Geology, v. 19, p. 211–214.
Fertl, W. H., 1976, Abnormal Formation Pressures: New York, Elsevier, 382 p.
Freeze, R. A., and Witherspoon, P. A., 1967, Theoretical analysis of regional groundwater flow. 2. Effect of water table configuration and subsurface permeability variation: Water Resources Research, v. 3, p. 623–634.
Garven, G., Ge, S., Person, M. A., and Sverjensky, D. A., 1993, Genesis of stratabound ore deposits in the midcontinent basins of North America. 1. The role of regional groundwater flow: Americanm Journal of Science, v. 293, p. 497–568.
Ge, S., and Garven, G., 1992, Hydromechanical modeling of tectonically driven groundwater flow with application to the Arkoma foreland basin: Journal of Geophysical Research, v. B97, p. 9119–9144.
Gratz, A. J.., 1991, Solution-transfer compaction of quartzites: Progress toward a rate law: Geology, v. 19, p. 901–904.
Greenberg, J. A., ms, 1971, Diffusional flow of salt and water in soils: Ph.D. thesis, University of California at Berkeley, 231 p.
Gretener, P. E., and Feng, Z., 1985, Three decades of geopressures—insights and enigmas: Bulletin der Vereinigung Schweiz. Petroleum-Geologen und -Ingenieure, v. 51, p. 1–34.
Gustafsson, P., 1994, SPOT satellite data for exploration of fractured aquifers in a semi-arid area in southeastern Botswana: Applied Hydrogeology, v. 2, p. 9–18.
Habermehl, M. A., 1980, The Great Artesian Basin, Australia: BMR Journal of Australian Geology & Geophysics, v. 5, p. 9–38.
Hanshaw, B. B., and Hill, G. A., 1969, Geochemistry and hydrodynamics of the Paradox Basin region, Utah, Colorado, and New Mexico: Chemical Geology, v. 4, p. 263–294.
Hanson, R. B., 1992, Effects of fluid production on fluid flow during regional and contact metamorphism: Journal of Metamorphic Petrology, v. 10, p. 87–97.
Harrison, W. J., and Summa, L. L., 1991, Paleohydrology of the Gulf of Mexico Basin: American Journal of Science, v. 291, p. 109–176.
Hitchon, B., 1969a, Fluid flow in the western Canada sedimentary basin, 1. Effect of topography: Water Resources Research, v. 5, p. 186–195.
———— 1969b, Fluid flow in the western Canada sedimentary basin, 2. Effect of geology: Water Resources Research, v. 5, p. 460–469.
Hubbert, M. K., and Rubey, W. W., 1959, Role of fluid pressure in mechanics of overthrust faulting, I. Mechanics of fluid-filled porous solids and its application to overthrust faulting: Geological Society of America Bulletin, v. 70, p. 115–166.
Hunt, J. M., 1990, Generation and migration of petroleum from abnormally pressured fluid compartments: American Association of Petroleum Geologists Bulletin, v. 74, p. 1–12.
Kreitler, C. W., Akhter, M. S., Donnelly, C. A., and Wood, W. T., 1988, Hydrogeology of formations used for deep well injection, Texas Gulf Coast: Austin, Texas Bureau of Economic Geology, 204 p.
Land, L. S., 1991, Evidence for vertical movement of fluids, Gulf Coast sedimentary basin: Geophysical Research Letters, v. 18, p. 919–922.
Magara, K., 1968, Subsurface fluid pressure profile, Nagaoka Plain, Japan: Bulletin of the Japan Petroleum Institute, v. 10, p. 1–7.
———— 1974, Compaction, ion filtration, and osmosis in shale and their significance in primary migration: American Association of Petroleum Geologists Bulletin, v. 58, p. 283–290.
Marine, I. W., and Fritz, S. J., 1981, Osmotic model to explain anomalous hydraulic heads: Water Resources Research, v. 17, p. 73–82.
McMahon, P. B., Chapelle, F. H., Falls, W. F., and Bradley, P. M., 1992, Role of microbial processes in linking sandstone diagenesis with organic-rich clays: Journal of Sedimentary Petrology, v. 62, p. 1–10.
Mitchell, J. K., Greenberg, J. A., and Witherspoon, P. A., 1973, Chemico-osmotic effects in fine-grained soils: Proceedings of the American Society of Civil Engineers, v. SM99, p. 307–322.
Mitchell, J. K., and Younger, J. S., 1967, Abnormalities in hydraulic flow through fine-grained soils: American Society for Testing and Materials, Special Technical Publication 417, p. 106–141.

Moline, G. R., Bahr, J. M., Drzewiecki, P. A., and Shepherd, L. D., 1992, Identification and characterization of pressure seals through the use of wireline logs: A multivariate statistical approach: Log Analyst, July-August, p. 362–372.

Mueller, S., and Landisman, M., 1966, Seismic studies of the Earth's crust in continents, I: Evidence for a low-velocity zone in the upper part of the lithosphere: Geophysical Journal of the Royal Astronomical Society, v. 10, p. 525–537.

Neuzil, C. E., 1985, Comment on "Possible effects of erosional changes of the topographic relief on pore pressure at depth" by J. Tóth and R. F. Millar: Water Resources Research, v. 21, p. 895–898.

——— 1986, Groundwater flow in low-permeability environments: Water Resources Research, v. 22, p. 1163–1195.

——— 1993, Low fluid pressure within the Pierre Shale; A transient response to erosion: Water Resources Research, v. 29, p. 2007–2020.

——— 1994, How permeable are clays and shales?: Water Resources Research, v. 30, p. 145–150.

Neuzil, C. E., and Pollock, D. W., 1983, Erosional unloading and fluid pressures in hydraulically "tight" rocks: Journal of Geology, v. 91, p. 179–193.

Norton, D. L., 1990, Pore fluid pressure near magma chambers, *in* Bredehoeft, J. D., and Norton, D. L., editors, The Role of Fluids in Crustal Processes: Washington, D. C., National Academy Press, p. 42–49.

Nur, A., and Simmons, G., 1969, The effect of saturation on velocity in low porosity rocks: Earth and Planetary Science Letters, v. 7, p. 183–193.

Nur, A., and Walder, J., 1990, Time-dependent hydraulics of the Earth's crust, *in* Bredehoeft, J. D., and Norton, D. L., editors, The Role of Fluids in Crustal Processes: Washington, D. C., National Academy Press, p. 113–127.

Oelkers, E. H., Bjorkum, P. A., and Murphy, W. M., 1992, A combined diffusion/kinetic/thermodynamic framework for the prediction of porosity reduction in sedimentary basin sandstones over geologic timeframes [abstract]: Geological Society of America Abstracts with Programs, v. 24, p. A327.

Olsen, H. W., 1972, Liquid movement through kaolinite under hydraulic, electric, and osmotic gradients: American Association of Petroleum Geologists Bulletin, v. 56, p. 2022–2088.

Ottman, J. D., 1984, Evolution of formation fluids in the "J" Sandstone, Denver Basin, Colorado, *in* Jorgenson, D. G., and Signor, D. C., Proceedings of the First C. V. Theis Conference on Geohydrology: Worthington, Ohio, National Water Well Association, p. 77–87.

Palciauskas, V. V., and Domenico, P. A., 1982, Characterization of drained and undrained response of thermally loaded repository rocks: Water Resources Research, v. 18, p. 281–290.

——— 1989, Fluid pressures in deforming porous rocks: Water Resources Research, v. 25, p. 203–213.

Peterson, E. W., Lagus, P. L., and Lie, K., 1987, WIPP horizon free fluid transport characteristics: Albuquerque, New Mexico, Sandia National Laboratory, Sandia Report SAND87-7164, 96 p.

Pfiffner, O. A., and Ramsay, J. G., 1982, Constraints on geological strain rates: Arguments from finite strain states of naturally deformed rocks: Journal of Geophysical Research, v. B87, p. 311–321.

Powley, D. E., 1990, Pressures and hydrogeology in petroleum basins: Earth-Science Reviews, v. 29, p. 215–226.

Pritchett, W. C., 1980, Physical properties of shales and possible origin of high pressures, Society of Petroleum Engineers Journal, v. 20, p. 341–348.

Rehm, B., 1972, Worldwide occurrence of abnormal pressures, Part II, Third Symposium on Abnormal Subsurface Pore Pressure: Dallas, Texas, Society of Petroleum Engineers, p. 43–50.

Rice, J. R., and Cleary, M. P., 1976, Some basic stress diffusion solutions for fluid-saturated elastic porous media with compressible constituents: Reviews of Geophysics and Space Physics, v. 14, p. 227–241.

Russell, W. L., 1972, Pressure-depth relations in Appalachian region: American Association of Petroleum Geologists Bulletin, v. 56, p. 528–536.

Screaton, E. J., Wuthrich, D. R., and Dreiss, S. J., 1990, Permeabilities, fluid pressures, and flow rates in the Barbados ridge complex: Journal of Geophysical Research, v. B95, p. 8997–9007.

Sharp, J. M., Jr., and Domenico, P. A., 1976, Energy transport in thick sequences of compacting sediment: Geological Society of America Bulletin, v. 87, p. 390–400.

Spencer, C. W., 1987, Hydrocarbon generation as a mechanism for overpressuring in Rocky Mountain Region: American Association of Petroleum Geologists Bulletin, v. 71, p. 368–388.
Stephenson, L. P., Plumley, W. J., and Palciauskas, V. V., 1992, A model for sandstone compaction by grain interpenetration: Journal of Sedimentary Petrology, v. 62, p. 11–22.
Šuklje, L., 1969, Rheological Aspects of Soil Mechanics: New York, John Wiley & Sons, 571 p.
Taylor, H. P., Jr., 1990, Oxygen and hydrogen isotope constraints on the deep circulation of surface waters into zones of hydrothermal metamorphism and melting, *in* Bredehoeft, J. D., and Norton, D. L., editors, The Role of Fluids in Crustal Processes: Washington, D. C., National Academy Press, p. 72–95.
Todd, T., and Simmons, G., 1972, Effect of pore pressure on the velocity of compressional waves in low-porosity rocks: Journal of Geophysical Research, v. 77, p. 3731–3743.
Tóth, J., 1963, A theoretical analysis of groundwater flow in small drainage basins: Journal of Geophysical Research, v. 68, p. 4795–4812.
——— 1981, Reply to Kinji Magara including a discussion of the "tensiometer effect' in cross-formational gravity-flow systems of formation fluids: Bulletin of Canadian Petroleum Geology, v.29, p. 134–142.
Tóth, J., Maccagno, M. D., Otto, C. J., and Rostron, R. J., 1991, Generation and migration of petroleum from abnormally pressured compartments: Discussion: American Association of Petroleum Geologists Bulletin, v. 75, p. 331–335.
Tóth, J., and Millar, R. F., 1983, Possible effects of erosional changes of topographic relief on pore pressures at depth: Water Resources Research, v. 19, p. 1585–1597.
Trimmer, D., Bonner, B., Heard, H. C., and Duba, A., 1980, Effect of pressure and stress on water transport in intact and fractured gabbro and granite: Journal of Geophysical Research, v. B85, p. 7059–7071.
Unruh, J. R., Davisson, M. L., Criss, R. E., and Moores, E. M., 1992, Implications of perennial saline springs for abnormally high fluid pressures and active thrusting in western California: Geology, v. 20, p. 431–434.
Vinard, P., Blumling, P., McCord, J. P., and Aristorenas, G., 1993, Evaluation of hydraulic underpressures at Wellenberg, Switzerland: International Journal of Rock Mechanics and Mining Science, v. 30, p. 1143–1150.
Vrolijk, P., Fisher, A., and Gieskes, J., 1991, Geochemical and geothermal evidence for fluid migration in the Barbados accretionary prism (ODP Leg 110): Geophysical Research Letters, v. 18, p. 947–950.
Walder, J., and Nur, A., 1984, Porosity reduction and crustal pore pressure development: Journal of Geophysical Research, v. B89, p. 11,539–11,548.
Walther, J. V., and Orville, P. M., 1982, Volatile production and transport in regional metamorphism: Contributions to Mineralogy and Petrology, v. 79, p. 252–257.
Weedmen, S. D., Guber, A. L., and Engelder, T., 1992, Pore pressure variation within the Tuscaloosa trend: Morganza and Moore-Sams fields, Louisiana Gulf Coast: Journal of Geophysical Research, v. B97, p. 7193–7202.